NOVEL EXPERIMENTAL STUDIES FOR COAL LIQUEFACTION: QUARTERLY PROGRESS REPORT, OCTOBER 1, 1987-DECEMBER 31, 1987

PITTSBURGH UNIV., PA

1987

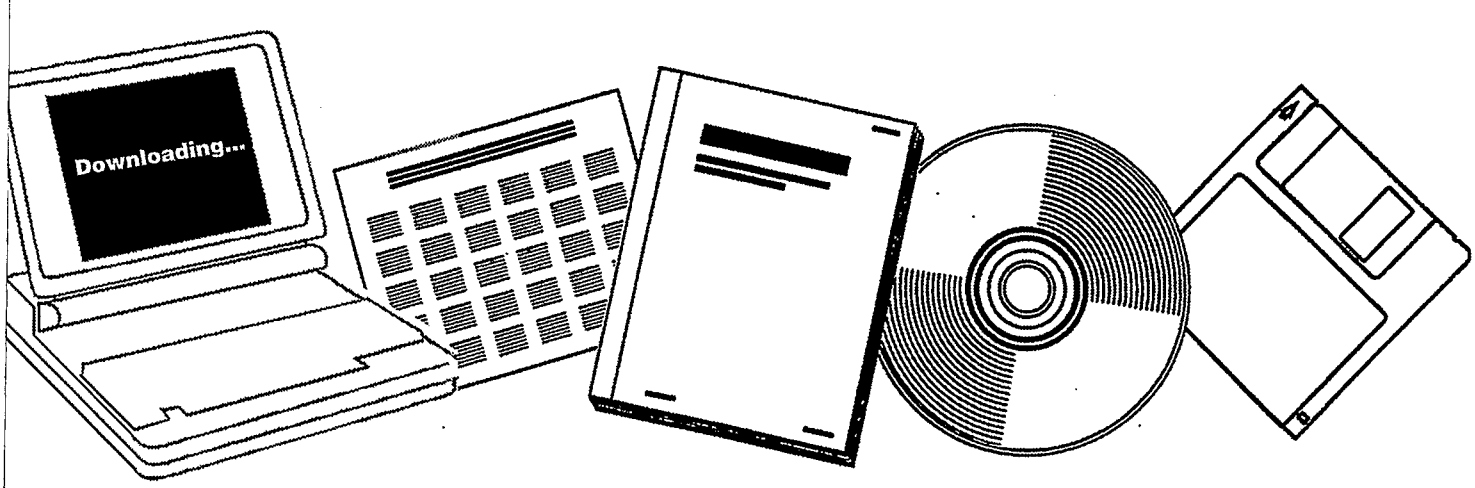

One Source. One Search. One Solution.

NTIS

Providing Permanent, Easy Access to U.S. Government Information

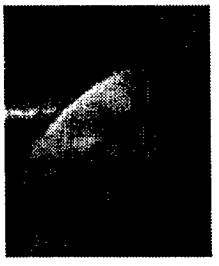

National Technical Information Service is the nation's largest repository and disseminator of government-initiated scientific, technical, engineering, and related business information. The NTIS collection includes almost 3,000,000 information products in a variety of formats: electronic download, online access, CD-ROM, magnetic tape, diskette, multimedia, microfiche and paper.

Search the NTIS Database from 1990 forward

NTIS has upgraded its bibliographic database system and has made all entries since 1990 searchable on **www.ntis.gov.** You now have access to information on more than 600,000 government research information products from this web site.

Link to Full Text Documents at Government Web Sites

Because many Government agencies have their most recent reports available on their own web site, we have added links directly to these reports. When available, you will see a link on the right side of the bibliographic screen.

Download Publications (1997 - Present)

NTIS can now provides the full text of reports as downloadable PDF files. This means that when an agency stops maintaining a report on the web, NTIS will offer a downloadable version. There is a nominal fee for each download for most publications.

For more information visit our website:

www.ntis.gov

U.S. DEPARTMENT OF COMMERCE
Technology Administration
National Technical Information Service
Springfield, VA 22161

LEGIBILITY NOTICE

A major purpose of the Technical Information Center is to provide the broadest dissemination possible of information contained in DOE's Research and Development Reports to business, industry, the academic community, and federal, state and local governments.

Although a small portion of this report is not reproducible, it is being made available to expedite the availability of information on the research discussed herein.

Quarterly Progress Report

DOE/PC/71257--T14
DE88 006827

NOVEL EXPERIMENTAL STUDIES FOR COAL LIQUEFACTION

Gerald D. Holder
John W. Tierney

University of Pittsburgh
Pittsburgh, PA 15261

Prepared for the Department of Energy
Contract No. De-FG22-84PC71257

October 1, 1987 to December 31, 1987

DISCLAIMER

NOVEL EXPERIMENTAL STUDIES FOR COAL LIQUEFACTION

Research is being carried out in this project in two areas which are of interest to ongoing investigations at the Pittsburgh Energy Technology Center (PETC). They are: (a) behavior of slurry reactors used for indirect coal liquefaction, and (b) coal liquefaction under supercritical conditions. The current status of each of these tasks is summarized in this report.

CONTENTS

LIST OF FIGURES

LIST OF TABLES

TASK 1: BEHAVIOR OF SLURRY REACTORS USED FOR INDIRECT COAL LIQUEFACTION

The conversion of synthesis gas to liquid products is usually carried out with the reactants in the gas phase and a solid catalyst. Because of relatively poor heat transfer from the gas to the solid, the exothermic heat of reaction is difficult to remove, and care must be taken to prevent the catalyst from overheating with loss of selectivity and activity. Slurry reactors in which the catalyst is suspended in a liquid medium and the gases are bubbled through the slurry have intrinsically better heat transfer characteristics and appear promising for indirect liquefaction processes.

1.1 Scope of Work

Experimental work is presently being concentrated on a two-step synthesis of methanol from CO and H_2. The process consists in the carbonylation of a molecule of methanol to methyl formate followed by hydrogenation to form two molecules of methanol. The kinetics of the individual reactions were first studied and the results have been included in previous progress reports. They are also presented in a paper which has been accepted for publication in Fuel Processing Technology. Subsequently, the two reactions were carried out concurrently -- both reactions taking place simultaneously in a single reactor. The concurrent reaction is very promising and we are concentrating experimental work in Task 1 on further elucidation of the effect of important design parameters.

A modeling study is also being carried out by Dr. Y. T. Shah at the University of Tulsa. He is investigating the non-isothermal unsteady state Fischer-Tropsch reaction. Experimental work which was begun on a previous project and which was

extended on this project demonstrated that multiple steady states can exist for this reaction.[1]

1.2 Results and Highlights

Experimental work and data analysis for the two-step concurrent synthesis of methanol were continued during the last quarter. As pointed out in the previous report, carrying out both reactions concurrently gives different results than predicted from knowledge of the individual reactions. One explanation is the existence of an interaction between the two catalysts. Since one catalyst is homogeneous and the other heterogeneous, the interaction could be adsorption of the homogeneous catalyst on the heterogeneous one. The extent of adsorption at room temperature was measured and found to be signficant.

Measurements of mass transfer coefficients from gas phase to liquid phase for systems containing H_2, CO, methanol and methyl formate were made to verify that the reaction rate data being obtained are not influenced by mass transfer limitations. It was found that mass transfer rates in the experimental reactor are at least 1000 times larger than reaction rates and hence are not rate limiting. Modeling of the unsteady state slurry phase Fischer-Tropsch reaction continued.

1.3 Future Work

During the next quarter, experimental work will include a study of in situ activation of the heterogeneous catalyst and further measurements of the effect of the H_2/CO ratio on reaction rate for the concurrent reaction. Work will continue on modeling of the Fischer-Tropsch reaction in a slurry reactor, and preparation of the final report for the project will begin.

1.4 Investigation of Catalyst Interaction

As noted in previous quarterly reports, there are significant differences in the behavior of the two-step synthesis when it is carried out concurrently as compared to carrying out the two reactions independently. We found that the reaction rate is higher than predicted and the inhibitory effect of CO and CO_2 on the reaction is greatly reduced. It appears that there is an interaction between the homogeneous catalyst used in the first step (potassium methoxide, MeOK) and the heterogeneous catalyst used in the second step (United Catalyst G-89, copper chromite with 1-5% manganese).

A likely form for the interaction is adsorption of MeOK on the solid catalyst. Once adsorbed on the surface, the MeOK could change the course of reaction in at least two ways.

1. The carbonylation reaction would become concentrated in the region near the heterogeneous catalyst surface because there is a high concentration of homogeneous catalyst near the sites where the MeF is disappearing because of reaction with H_2 and where equilibrium will favor the carbonylation reaction. This would deplete the region near the surface of CO and thus offset the known deleterious effect of CO on the hydrogenation reaction. The magnitude of the depletion would depend on the rate of diffusion of CO from the bulk liquid to the catalyst surface. For very small catalyst particles such as used in this work (average size, 2 microns), diffusion should be very rapid, and this effect is not expected to be large.
2. The adsorbed MeOK could serve to remove CO and CO_2 from the catalyst surface by competing for the same adsorption sites or by reaction with adsorbed CO.

In order to determine whether MeOK was adsorbed on the hydrogenation catalyst, a solution of MeOK and MeOH (0.00476 gm MeOk/gm solution) was charged to the reactor at room temperature and pressure. Next, about 3 grams of G-89 catalyst were reduced outside the reactor and then added to the reactor. The mixture was stirred at room temperature for one hour and then removed from the reactor and allowed to settle out. The supernatant liquid was decanted and titrated for MeOK using a 0.1 N HCl solution. The concentration of MeOK was unchanged as expected since a very small amount of catalyst was used. The catalyst and adhering liquid were removed and weighed. It was then washed three times to remove MeOK and then dried and weighed. The amount of MeOK in the wash liquid was determined by titration. Since the amount of liquid adhering to the solid was known from the measured weights and since the concentration of MeOK in this liquid must be the same as in the supernatant liquid, the MeOK on the catalyst surface could be calculated. The result is an equilibrium concentration of 0.00355 gm MeOK/gm catalyst for a solution concentration of 0.00476 gm MeOK/gm solution. It is improtant to note that these measurements were made at room temperature. Additional measurements should be made at reaction conditions. It is evident, however, that signficant adsorption of MeOK on the catalyst surface does occur.

1.5 Measurement of Mass Transfer Coefficients of H_2 and CO

In order to obtain intrinsic reaction kinetic data, it is necessary that the interphase mass transfer resistances are small compared to the reaction resistances. In a three phase slurry reactor, the mass transfer resistance between the gas and the liquid phases is usually much larger than that between the liquid and solid phase. For particles less than 40 μm, the reaction may occur predominantly on the outer

surface.[2] The diffusion resistance in the catalyst pores is expected to be small because catalyst particles used in this work are of the order of 2 microns. To minimize gas-liquid transfer resistance in this work, high stirring speeds have been used. Estimates and some preliminary measurements made early in this project indicated that mass tranfer rates should not be limiting. An experimental verification was carried out during the last quarter.

The relation between reaction rate and mass transfer coefficient can be developed using the carbonylation of methanol for which the forward reaction rate can be expressed as:

$$r_r = k_r C_{CO} C_{Cat} C_{MeOH} \quad (3)$$

where k_r is the intrinsic reaction rate constant, C_{CO}, C_{Cat} and C_{MeOH} are concentrations of CO, catalyst and methanol. The mass transfer rate of CO from the gas phase to the liquid phase can be written as:

$$r_m = K_L a(C_{CO,e} - C_{CO}) \quad (4)$$

where $K_L a$ is the overall gas-liquid mass transfer coefficient and $C_{CO,e}$ is the equilibrium CO concentration. These two rates are identical at steady state conditions. The reaction rate equation 3 can then be written in terms of $C_{CO,e}$ instead of C_{CO} which was not measured.

$$r_r = k_r [K_L a/(k_r C_{Cat} C_{MeOH} + K_L a)] C_{CO,e} C_{Cat} C_{MeOH} \quad (5)$$

The term in the square brackets of equation 5 is a coefficient which measures how far the CO concentration, C_{CO}, is from the equilibrium value, $C_{CO,e}$. This coefficient varies from zero to one. For example, under conditions such that the mass transfer coefficient K_La is much larger than the reaction rate term, $k_rC_{Cat}C_{MeOH}$, the coefficient approaches 1 and the real CO concentration in the liquid equals the equilibrium value.

Comparing equation 5 to the rate equation we developed for the forward carbonylation reaction:

$$r_r = K_rC_{Cat}C_{MeOH}P_{CO} =$$
$$k_r[K_La/(k_rC_{CAT}C_{MeOH} + K_La)]\ H\ C_{CO,e}C_{Cat}C_{MeOH} \qquad (6)$$

the coefficient in the square brackets of equation 5 is included in the reaction rate constant, K_r. If the coefficient in the square brackets is 1, the apparent reaction rate constant K_r equals the intrinsic reaction rate constant. Otherwise, the apparent reaction rate constant obtained would be smaller than the intrinsic reaction rate constant.

The measurement of mass transfer coefficients of H_2 and CO in methanol and methyl formate was made in the same reactor used for studying the reaction. A batch gas adsorption technique was utilized. The reactor was first cleaned, charged with 500 cc of liquid (methanol or methyl formate) and then sealed. After the temperature of the reactor reached the desired value and stabilized, the stirrer was turned off. A gas (H_2 or CO) was then slowly introduced into the reactor from the top until the pressure equalled 250 psig. The temperature and the pressure of the reactor stabilized in about 2 to 5 minutes. The stirrer was then turned on. The total pressure of the reactor decreased with time because the gas dissolved. The

change of pressure was measured with a pressure transducer (Setra 205-2) and recorded with a chart recorder (HP-7702B). The initial slope of the pressure-time curves was used to calculate the mass transfer coefficient, K_La, with the assumption that at the initial time the gas concentration in the liquid is zero. The experiments were carried out at different stirrer speeds and temperatures. The results are shown in Figure 1-1 to 1-4. A comparison of the apparent and the intrinsic reaction rate constant for the forward carbonylation reaction is shown in Table 1. It is clear that mass transfer is not a limiting step for the carbonylation reaction. Comparison of K_La for H_2 in methyl formate to the hydrogenolysis rate, and K_La for H_2 and CO in methanol to the concurrent two step reaction rate shows that the mass transfer coefficients are at least 1000 times larger than the reaction rate terms. It is evident that for kinetic data reported previously in this project, the controlling step are reactions and the reported kinetic data are intrinsic.

1.6 Modeling of Non-Isothermal Fischer-Tropsch Slurry Reactors

This work is being done at the Unviersity of Tulsa by Dr. Y. T. Shah. The object is to investigate interactions among the Fischer-Tropsch reactions, the thermal effects, and the water gas shift reaction. The coupling of these phenomena has not been addressed in the published literature. The basic reactions which occur in the Fischer-Tropsch synthesis were presented in the July-September quarterly report. During the last quarter, the equations were put into non-dimensional form, ranges of values for the model parameters were evaluated, and a computer program for solution of the equations was written.

There are eleven simultaneous equations which describe the reacting system. These are four gas phase material balance equations, five liquid phase material balances, an overall material balance, and an energy balance. The solution is

complicated by the fact that multiple solutions are possible, and one of the main objectives of the study is to delineate conditions under which multiple solutions can exist. The solution method is based on the method proposed by Hoffman et al.[3] One of the variables (the reaction temperature) is assumed. The energy balance equation is removed from the set of equations, and the remaining equations are solved simultaneously. The energy being removed from the reactor (principally via flow of product streams) is calculated, and the heat generation in the reactor is calculated. These are not, in general, equal. The calculations are repeated for a series of assumed temperatures, and a plot is made of heat generation and heat removal versus temperature, and crossings on the plots indicate the temperatures for steady states. There will be multiple crossings if multiple steady states can exist. Using typical values, some solutions have been obtained. Work will continue during the next quarter to test the program and the computation method.

Bibliography

1. Bhattacharjee, S., J. Tierney, and Y.T. Shah, "Thermal Behavior of a Slurry Reactor: Application to Synthesis Gas Conversion," I&EC Process Design and Development, 25, 117(1986).
2. Chaudhari, R.V. and Ramachandran, P.S., "Three Phase Slurry Reactors," AIChE J., Vol. 26, No. 2, 1980, pp. 185.
3. Hoffman, L.A., S. Sharma, and D. Luss, "Steady State Multiplicity of Adiabatic Reactors," AIChE J., 21, 318(1975).

Nomenclature

C_{cat}: concentration of catalyst in the liquid, mol/L

C_{CO}: concentration of CO in the liquid, mol/L

$C_{co,e}$: equilibrium concentration of CO in the liquid, mol/L

C_{MeOH}: concentration of methanol in the liquid, mol/L

H: solubility constant, $H = \frac{P_{co}}{C_{co,e}}$, atm.L/mol.

K_La: volumetric mass transfer coefficient, 1/min

k_r: intrinsic reaction rate constant, $L^2/mol^2 \cdot min$

K_r: apparent reaction rate constant, $L^2/mol^2 \cdot min$

r_m: mass transfer rate, mol/L·min

r_r: reaction rate, mol/L·min

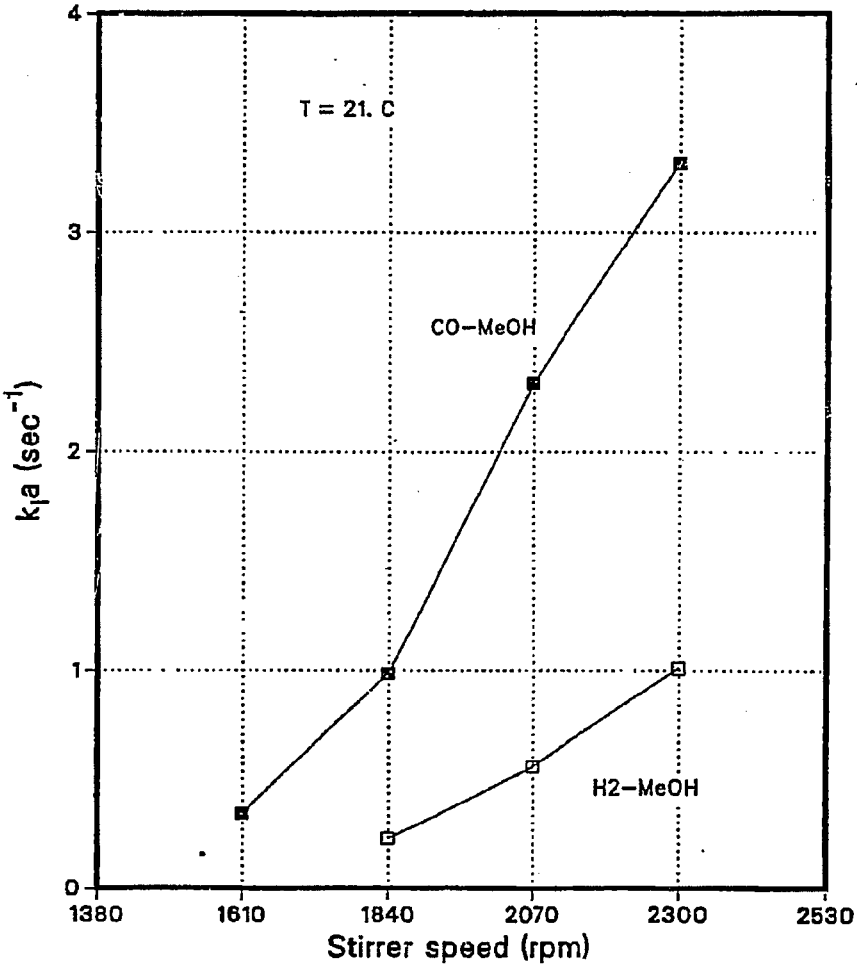

Figure 1-1. Gas-liquid mass transfer coefficient for H_2 and CO in methanol. Effect of stirrer speed at 21°C.

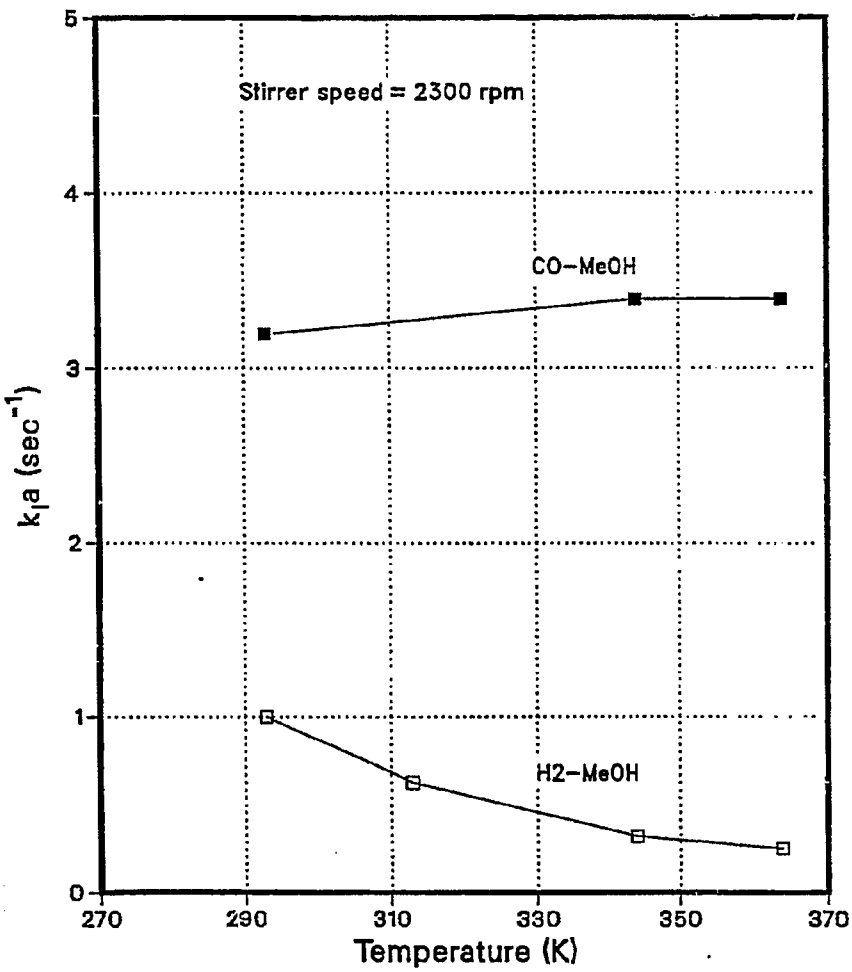

Figure 1-2. Gas-liquid mass transfer coefficient for H_2 and CO in methanol. Effect of temperature at 2300 rpm.

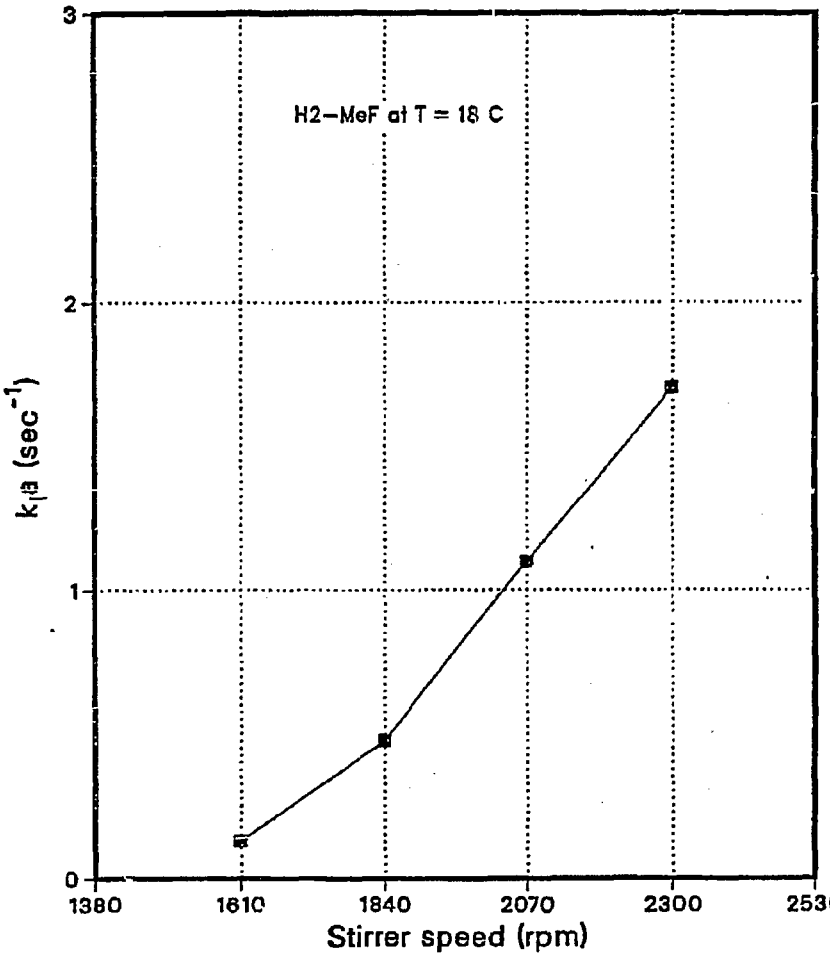

Figure 1-3. Gas-liquid mass transfer coefficient for H_2 in methyl formate. Effect of stirrer speed at 18°C.

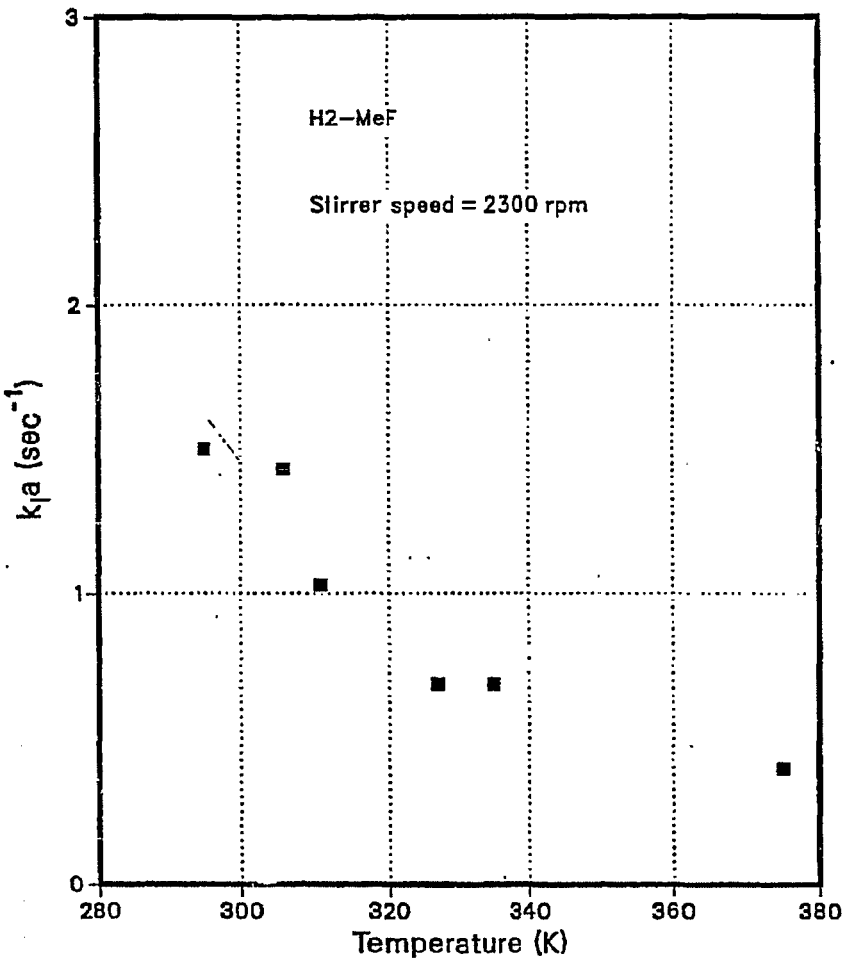

Figure 1-4. Gas-liquid mass transfer coefficient for H_2 in methyl formate. Effect of temperature at 2300 rpm.

TABLE 1-1

Comparison of Apparent and Intrinsic Rate Constant for Carbonylation of Methanol at Different Reaction Conditions and a Stirrer Speed of 2300 rpm

T (°C)	Reaction Rate Constant ($L^2 \cdot mol^{-2} \cdot min^{-1}$) Apparent	Intrinsic
114	3.44	3.76
102	1.76	1.84
94	1.09	1.13
86	0.67	0.67
85	0.63	0.64
83	0.55	0.56
82	0.52	0.52
81	0.49	0.49
80	0.45	0.46
71	0.25	0.25
61	0.12	0.12

TASK 2: COAL LIQUEFACTION UNDER SUPERCRITICAL CONDITIONS

Supercritical fluid extraction is an attractive process primarily because the density and solvent power of a fluid changes dramatically with pressure at near critical conditions, and during the extraction of coal, the density of a supercritical fluid should also change the extractability of the coal. During earlier quarters a non-reacting supercritical fluid, toluene, was studied to determine the effect of density on the coal extraction/reaction process. Extractions were carried out for 2 to 60 minutes at reduced densities between 0.5 and 2.0 and at temperatures between 647 and 698 K. The data obtained can be explained by the hypothesis that coal dissolution is required preceding liquefaction reactions and that the degree of dissolution depends upon solvent density and temperature. A kinetic model shows that higher solvent densities result in faster conversion rates and in higher total conversions. Two papers have resulted from this study.

A second factor that makes supercritical extraction attractive is high mass transfer rates. At high pressures, mass transfer rates in a supercritical fluid are much higher than in a liquid, despite the fact that the supercritical fluid has liquid-like solvent powers. The objective of this work is to measure mass transfer rates for naphthalene extraction by carbon dioxide to enable us to determine how mass transfer coefficients vary with pressure, flow rate, and bed height, since these parameters will influence the design of extraction or reaction processes which utilize supercritical fluids. Ultimately, such measurements will be extended to coal/supercritical fluid systems to help define the flow rates liquid/solvent ratios that would be appropriate for a supercritical system.

In this report, the entire program for evaluating mass transfer coefficients under supercritical conditions is described and a review of current knowledge and planned correlational approaches is given.

2.1 Background

Historically, interest in supercritical fluids was initially related to the observation that such fluids were often excellent solvents. This fact was discovered over 100 years ago by Hannay[12] and by Hannay and Hogarth.[13,14] Prior to that time, it was generally thought that materials above their critical temperatures would be gaseous in nature and thus poor solvents.

Studies of solubilities in supercritical fluids have been continued[15,16] and in most instances, they concentrated on developing phase diagrams for binary mixtures, particularly pressure-temperature projections. Vapor-liquid equilibrium data on binary hydrocarbon systems at elevated pressure became available in the 1930's[17,18] and the first patent for the practical application of supercritical extraction was made in 1943.[19] Later, Maddacks,[20] Tugrul[21] and Bartle et al.[22] described the extraction of components of low volatility from coal liquids using supercritical toluene. Barton and Fenske[23] suggested using C_{11} and C_{12} paraffinic fractions to desalinate sea water. Hubert and Vitzhu[24] studied on the removal of nicotine from tobacco leaves, of caffeine from green coffee beans, and the separation of a hop extract from commercial hops, in all cases using supercritical carbon dixoide. Modell et al.[25,26] discussed the regeneration of activated carbon by the use of supercritical carbon dioxide.

Critical data for a number of possible supercritical fluid solvents are listed in Table 2-1. These gases are suitable as a solvent either on their own or as components of mixtures. Because of their low critical temperatures, several of them can be used to extract heat-labile substances. Particularly, supercritical carbon dioxide is a very attractive solvent for practical applications because it is nonflammable, nontoxic, environmentally acceptable and relatively inexpensive. The critical temperature of carbon dioxide is only 304°K (31°C) and thus it can be used at moderate temperature for the extraction of heat sensitive substances

without degradation. One good example of using supercritical carbon dioxide is shown in selective extraction of caffeine from green coffee beans.

Table 2-1: Critical Data for Some Supercritical Solvents[79]

Substance	Critical Temperature K	Critical Pressure MPa	Critical Density g cm^{-1}
Methane	191	4.60	0.162
Ethylene	282	5.03	0.218
Chlorotrifluoro methane	302	3.92	0.579
Carbon dioxide	304	7.38	0.468
Ethane	305	4.88	0.203
Propylene	365	4.62	0.233
Propane	370	4.24	0.217
Ammonia	406	11.3	0.235
Diethyl ether	467	3.64	0.265
n. Pentane	470	3.37	0.237
Acetone	508	4.70	0.278
Methanol	513	8.09	0.272
Benzene	562	4.89	0.302
Toluene	592	4.11	0.292
Pyridine	620	5.63	0.312
Water	647	22.0	0.322

The supercritical fluid (SCF) region is not defined rigorously, but for the practical considerations, the SCF region is usually defined at conditions bounded approximately by $0.9 < T_r < 1.2$ and $P_r > 1.0$ where the SCF is very compressible as illustrated in Figure 2-1. For example, at a constant T_r of 1.0, increasing pressure from $P_r = 0.8$ to $P_r = 1.2$ significantly increases the density from gas-like densities to liquid-like densities. At higher reduced temperature, the pressure increase required to increase an equivalent density becomes greater. This practical consideration sets the upper bound on temperature. At higher pressures, the density is less sensitive to temperature changes. In the vicinity of the critical point, large density changes can be obtained with either relatively small pressure or temperature changes.

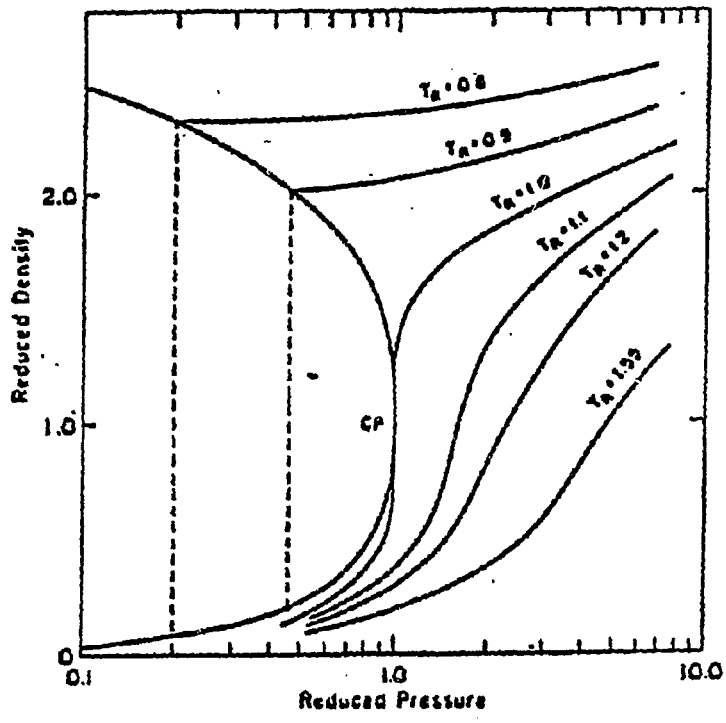

Figure 2-1: Reduced density-reduced pressure diagram for carbon dioxide at various reduced temperatures (T_r) in the vicinity of the critical point(CP) [35]

The effect of SCF solvent density on solubilities is shown directly in Figure 2-2 in the naphthalene-ethylene system.[27,28] Solubilities increase with increasing ethylene densities along each isotherm due to increasing solvent power, and with increasing temperature at constant density due to increasing volatility of naphthalene. These solvent properties vary continuously with solvent density and thus control solvent power and enhance the selectivity of the solvent. Also solvent and solute can be easily separated, and we can fractionate multiple solutes by stepwise reductions in solvent density.

In addition, SCF have better physicochemical properties than do gases and liquids. The order-of-magnitude comparison shown in Table 2-2 indicates that, while SCF has liquid-like densities, its viscosities and diffusivities are intermediate to those properties for liquids and gases. Thus SCF has the solvent power of liquids with better mass-transfer properties.

Table 2-2: Order of Magnitude Comparison of Gas, SCF and Liquid Phases[35]

Property	Gas	Phase SCF*	Liquid
Density (kg/m^3)	1	700	1000
Viscosity (Ns/M^2)	10^{-5}	10^{-4}	10^{-3}
Diffusion coefficient (cm^2/s)	10^{-1}	10^{-4}	10^{-5}

---

* At $T_r = 1$ and $P_r = 2$

** 10^3 centipoise = 1 Ns/m^2

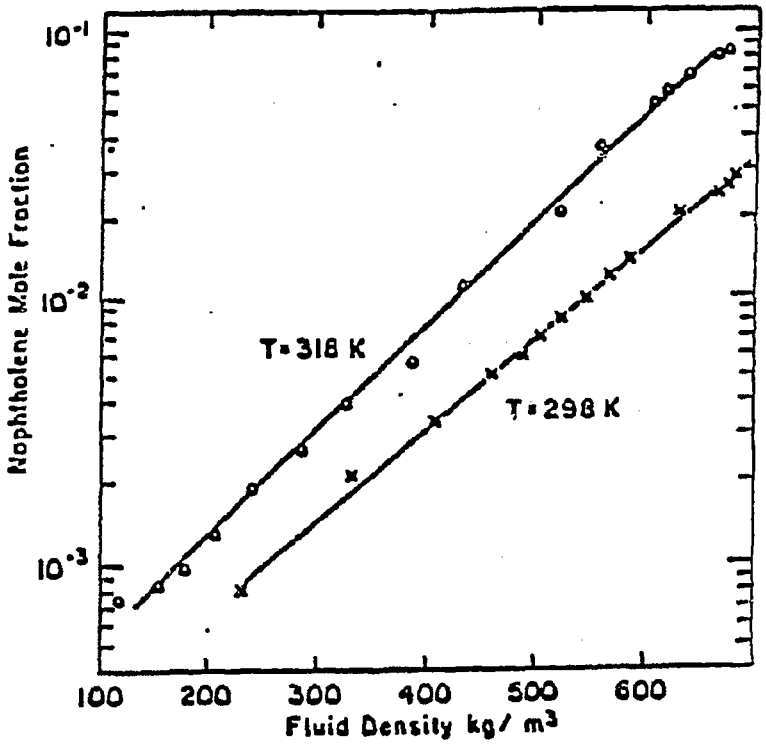

Figure 2-2: Solid solubilities of naphthalene in compressed ethylene as a function of ethylene density [35]

2.2 Diffusion Coefficient and Viscosity

The development of mass-transfer models requires knowledge of the diffusion coefficient of the solute, the viscosity, and the density of the fluid phase which can be used to correlate mass transfer coefficients.

Experimental data on diffusion coefficients in supercritical condition are scarce. Most studies on diffusion coefficient in the high pressure had been limited to the measurement of self diffusion coefficients, and binary diffusion coefficients in simple systems such as H_2-N_2, He-N_2 and H_2-Ar.[32] But recently, several experiments has been done to measure the diffusivities in systems such as naphthalene-CO_2,[33,34] benzene-CO_2 and caffeine-CO_2.[33] As a result of this work, it has been found that the viscosities and diffusivities of supercritical fluids were strongly dependent upon pressure and temperature in the vicinity of the critical point, and the ratios $(D_V\rho)/(D_V\rho)^o$ were 0.8 to 1.2. $(D_V\rho)^o$ is the value calculated on the basis of the low density theory for a gas at the given temperature. In the recent review article,[35] diffusion coefficient for the several systems were shown as a function of reduced pressure in Figure 2-3.

The viscosity of compressed fluids have been studied quite extensively. In Figure 2-4, the typical data of the viscosities of supercritical carbon dioxide is given as a function of pressure.[36] At the low pressure, the viscosities of carbon dioxide are essentially independent of pressure, but above the critical pressure, the viscosities increase rapidly with pressure.

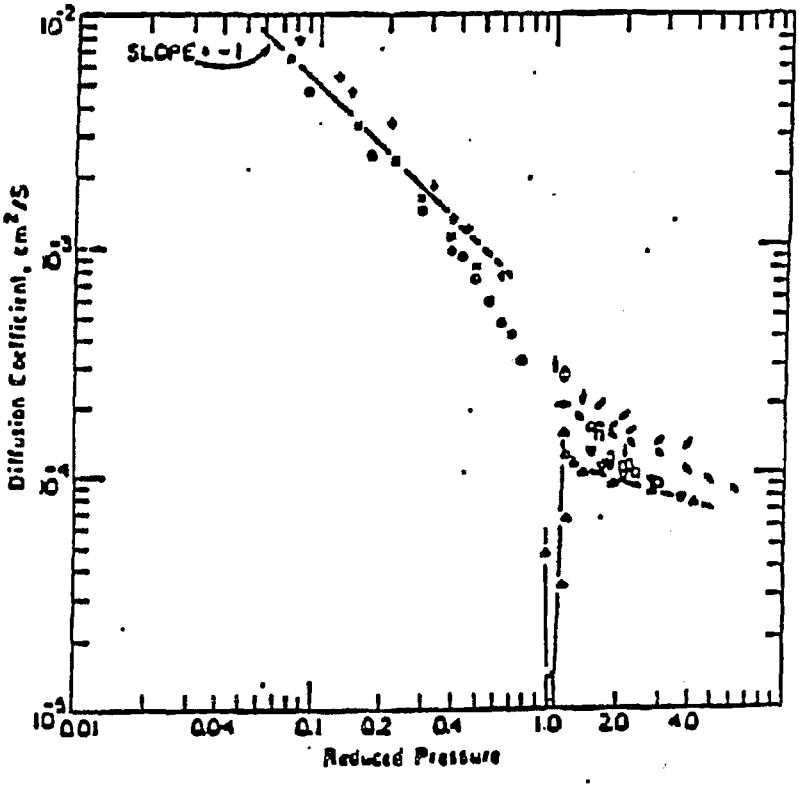

Figure 2-3: Diffusion coefficient in supercritical fluids [35]

Table 2-3: Key for figure 2-3.

Symbol	T, °C	System	Reference
•	30	CO_2-Naphthalene	36, 37
▪	30		
♦	40		
▲	35	CO_2-Naphthalene	38
▽	55		
/	13	Ethylene-Naphthalene	38
-·-	35		
|	40	CO_2-benzene	40
-·-	40	CO_2-Propylbenzene	34
○	40	CO_2-1,3,5-Trimethylbenzene	34

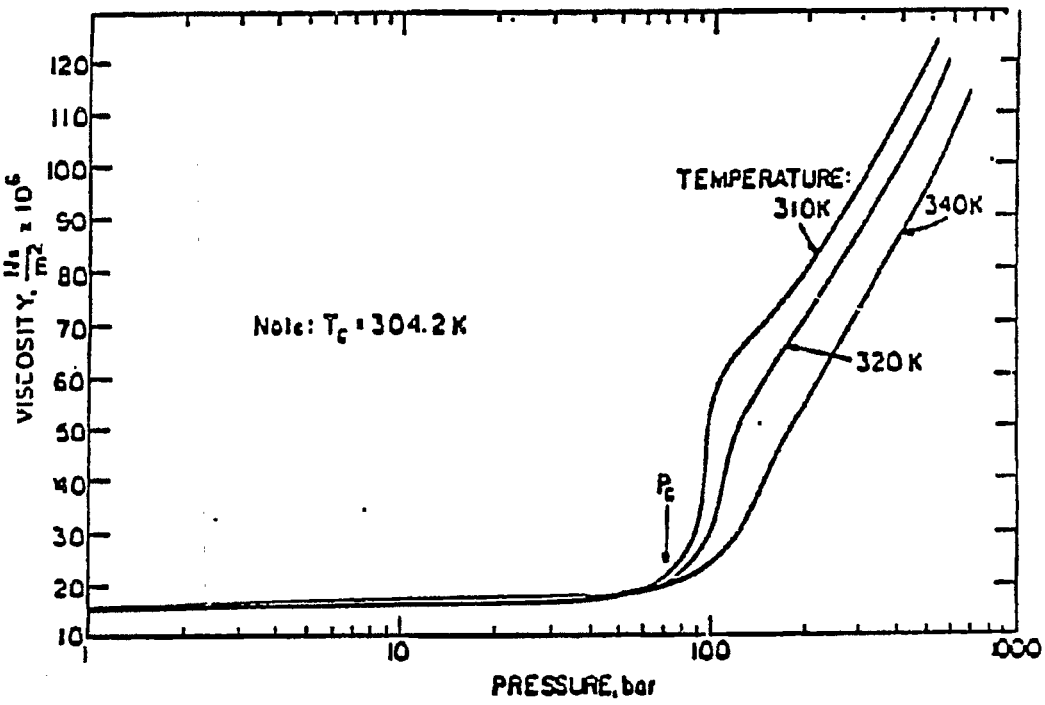

Figure 2-4: Viscosity of supercritical carbon dioxide[35]

2.3 Models for Flow System in a Packed Bed

The packed bed reactor is applicable in many operations, such as extraction, adsorption, leaching, ion exchange and catalytic processes. Therefore, mass-transfer coefficients in packed beds is the focus of the current research. First models for determining mass transfer from our experiments (past 38) will be developed and then these coefficients will be correlated.

The simplest flow model for the packed bed is the ideal plug flow model with no longitudinal mixing but complete radial mixing. Although no actual reactors can be fully represented by an ideal model, the plug flow model can be used in a number of packed bed reactors which behave close to the ideal.

However, flow behavior of most of the actual packed bed reactors deviates from ideal conditions. The deviation may be caused by nonuniform velocity profile, velocity fluctuation due to molecular or turbulent diffusion, by short-circuiting, by-passing and channeling of fluid, and by the presence of stagnant regions of fluid caused by the reactor shape and internals. Many flow models considering the nonideality of the flow pattern in packed reactor have been proposed.[37-41] Among them, the cell model or compartment model[40,41] is one of the most widely used models owing to its advantages over other models as decribed below. We used these two models (ideal plug flow model and cell model) to get mass-transfer coefficients and estimate nonideality.

The Ideal Plug Flow Model

Flow patterns in packed bed reactors with small ratios of the tube and particle diameter to length can be closely approximated by plug flow. The measurement of mass-transfer coefficients is based upon the following equation:

$$dN_A = d(V_T y_A) = k_y(y_A^* - y_A)dA = k_y(y_A^* - y_A)a_S S dL \tag{2-1}$$

Here,

$$V_T = \frac{1'}{1 - y_A} \tag{2-2}$$

where V' is molal flow rate of inert component in moles per unit time. Therefore,

$$d(V_T y_A) = V' d\left(\frac{y_A}{1 - y_A}\right) = v' \frac{dy_A}{(1 - y_A)^2} = V_T \frac{dy_A}{(1 - y_A)} \tag{2-3}$$

From equations (2-1) and (2-2)

$$\int_{y_{A,in=0}}^{y_{A,out}} \frac{dy_A}{(1 - y_A)(y_A^* - y_A)} = \frac{k_y a_S}{\bar{G}_{My}} \int_0^{L_T} dL \tag{2-4}$$

where $\bar{G}_{My}$ is the average molal mass velocity of the gas in moles per unit area per unit time. For dilute gas (i.e., $1 - y_A \approx 1$),

$$\int_0^{y_{A,out}} \frac{dy_A}{y_A^* - y_A} = \left(\frac{k_y a_S}{\bar{G}_{My}}\right) L_T \tag{2-5}$$

By integration and rearrangement,

$$k_y a_S = \left(\frac{\bar{G}_{My}}{L_T}\right) \ln \left(\frac{y_A^*}{y_A^* - y_{A,out}}\right)$$

Axial Dispersion in a Packed Bed

Several models have been used to analyze and correlate experimental data on mixing in a packed bed. They introduced radial and/or axial diffusion coefficients E_r and/or E_a, independent of solute concentration, to take into account the mixing effect in the radial and/or axial directions respectively, for packed beds. These diffusion coefficients can be realted to flow parameters, fluid properties and the geometry of the bed and the packing.

In a packed bed catalytic reactor, a chemical reaction takes place in a bed and heat flows through the tube wall and therefore, the radial heat and mass transfer are not negligible. However, radial dispersion can usually be neglected compared with axial dispersion when the ratio of column diameter to length is small and the flow is in the turbulent regime. Many investigators have found that the mixing effect in packed beds could be well described in an axial dispersion coefficient E_a alone even though there was some radial dispersion effect.

Dankwerts[41] first published the results on axial dispersion in a packed bed. Wen and Fan[42] summarized the results of previous investigations on the axial dispersion of liquids (Figure 2-5) and gases (Figure 2-6) in packed beds and have developed empirical correlations (shown below) based on about 500 data points for liquids and gases, respectively. The axial Peclet number $P_{e,a}$ is defined as $d_p u/E_a$. These equations can be used to determine the axial diffusion coefficient E_a for liquids and gases, respectively.

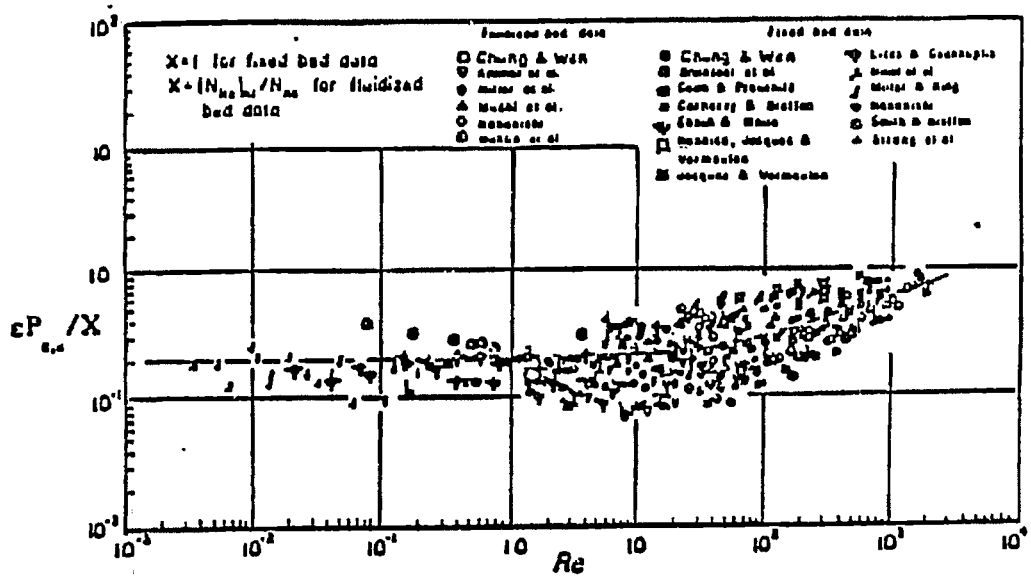

Figure 2-5: A Correlation of longitudinal dispersion coefficient of liquid phase fixed beds and fluidized beds in terms of peclet number[42]

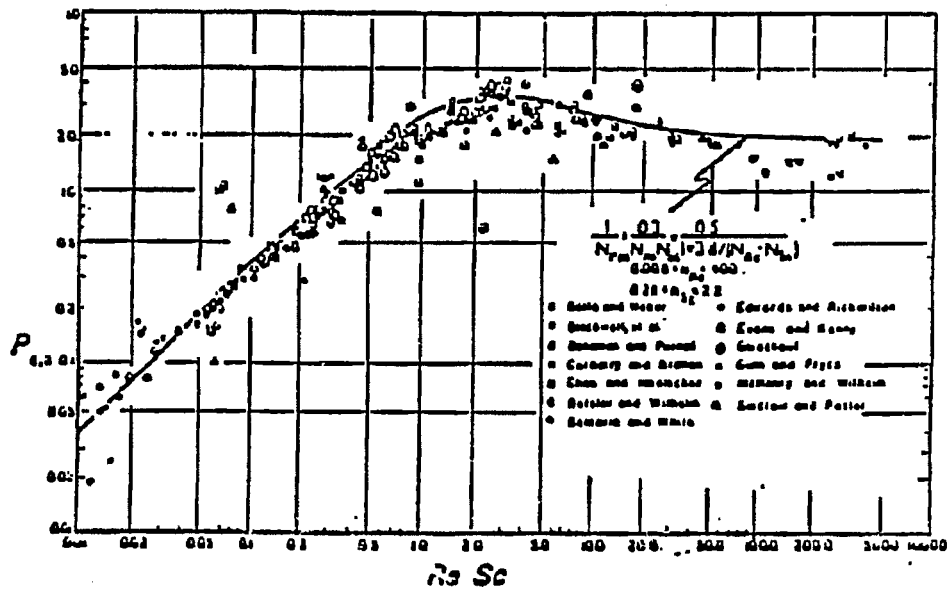

Figure 2-6: Correlation of axial dispersion coefficient for gases flowing through fixed beds[42]

Liquids:

$$\varepsilon P_{e,a} = 0.2 + 0.11\ Re^{0.48} \tag{2-7}$$

Gases:

$$\frac{1}{P_{e,a}} = \frac{0.3}{ScRe} + \frac{0.5}{1 + 3.8(ReSc)^{-1}} \tag{2-8}$$

for $0.008 < Re < 400$ and $0.28 < Sc < 2.2$

The general correlation of existing data of the axial dispersion coefficient for liquids and gases respectively[43] is shown in Figure 2-7. The dashed lines represent the molecular-diffusion asymptotes, for $Pe = (Re)(Sc)T_\varepsilon/\varepsilon$. The lines shown are for $T_\varepsilon = \sqrt{2}$ and $\varepsilon = 0.4$. In the case of gases, $P_{e,a}$ remains approximately constant, decreasing little from its value of 2 until molecular diffusion is important at Re around 1.0. Molecular diffusion in liquids, however, is so slow that E_a increases as Re is reduced below 500. But as Re is decreased from 300 to 10, $P_{e,a}$ remains approximately proportional to Re indicating that E_a is roughly constant in this region. The correction of $P_{e,a}$ with Re is greatly dependent on the magnitude of the molecular diffusion coefficient D_V, that is, Schmidt number $Sc = \mu/\rho D_V$.

Even though no experimental data on axial dispersion have been published for supercritical fluids, we can approximate its effect as described below. For supercritical systems, the value of the Schmidt number, around 10, is intermediate to the values for gases (Sc = 1.0) and liquids (Sc = 1000). By comparing the order of magnitude of Schmidt number for gases, supercritical fluids and liquids, we can assume that the value of $P_{e,a}$ for SCF is so close to the value of $P_{e,a}$ for gas and is approximately equal to 2.0 when Re is greater than 1.0.

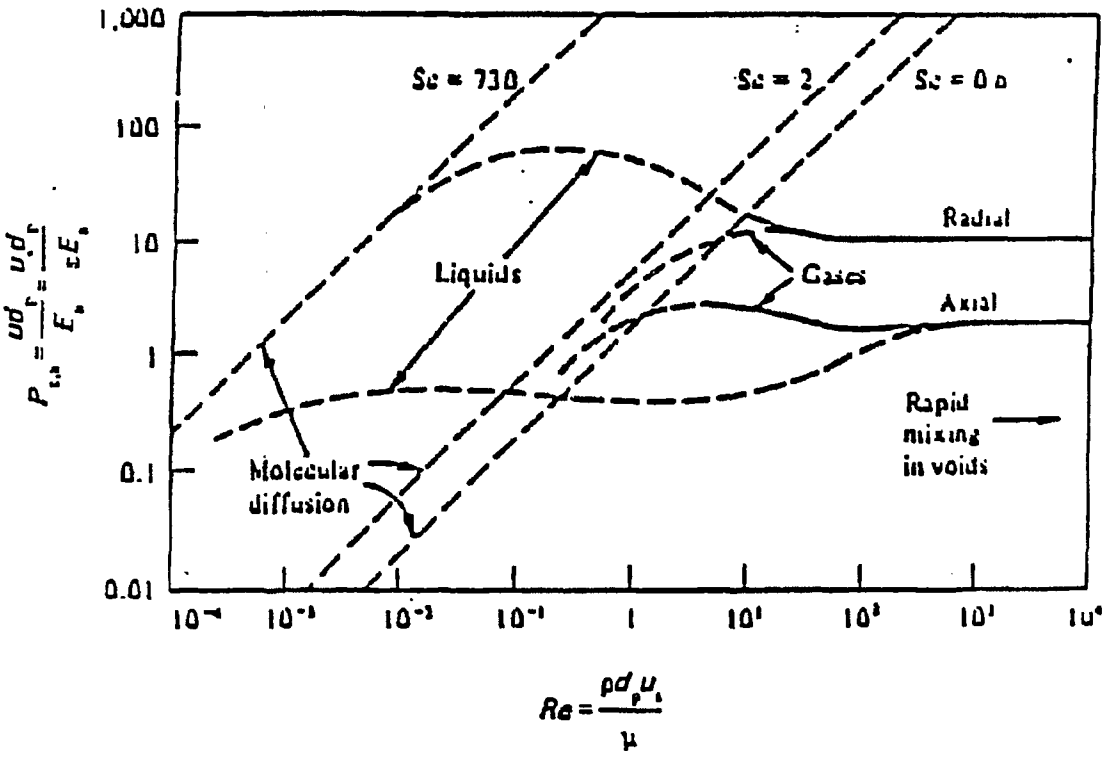

Figure 2-7: Approximate representation of a large amount of published data on radial and axial dispersion in randomly packed beds of uniform spheres: flow of a single phase [43]

Kramers and Alberda[44] first discussed an analogy between a packed bed and a series of mixing vessels. By an analogy between the mechanism of imperfect mixing and Einstein's kinetic diffusion model, Carberry[37] showed that the number of perfect mixing tanks, n is given by:

$$n = \frac{Lu}{2E_a} = \frac{L}{d_p}\frac{P_{e,a}}{2} \tag{2-9}$$

As $E_a \to \infty$ for n = 1.0, then for a small number of mixers less than 10:[44]

$$n - 1 = \frac{Lu}{2E_a} \tag{2-10}$$

These equations are used for determining the number of perfect mixers to be used in the cell model below.

Mass-Transfer Coefficient from the Cell Model

The cell model is a generalization of a class of models such as the completely mixed tanks-in-series model and the back-flow mixed tanks-in-series model. The common characteristic of this model is that the basic mixing unit is a completely mixed or stirred tank. This model has been employed extensively from early days of chemical engineering to the present.[40,41,45-48] This cell model has the following practical advantages over other models:

1. The transition mixing behavior of such model can be presented by a set of linear first-order ordinary differential equations instead of partial differential equations.
2. The steady-state reaction in such a model can be represented by a set of finite difference equations rather than differential equations.

Since complete mixing is assumed in a cell, the mole fraction of a solute in out-going stream from the ith cell is y_i. If the bed is viewed as a series of n perfect mixing cells each having surface area of pellets A_T/n and constant mass-transfer coefficient k_y, then for the steady-state mass-transfer the material balance around the first cell gives

$$k_y(A_T/n)(y^* - y_1) = V_T(y_1 - y_o) \tag{2-11}$$

Finally, we can obtain the following expression for n cells by using the similarity for each cell (its derivation is not given here)

$$k_y a_S = \frac{nV_T}{SL_T}\left[\left(\frac{y^* - y_o}{y^* - y_n}\right)^{1/n} - 1\right] \tag{2-12}$$

As mentioned above, we can assume that the value of $P_{e,a}$ for SCF is approximately equal to 2.0 when Re is greater than 1.0. Then, the number of perfect mixers in a packed bed can be determined by equation (2-9) or (2-10) depending upon the number of layers of the pellets in a packed bed (L/d_p). Finally, the mass-transfer coefficient under supercritical conditions can be obtained by equation (2-6) and/or (2-12) using the plug flow and/or cell models, respectively.

2.4 Mass-Transfer Correlations

After mass-transfer coefficients under supercritical conditions are determined, they need to be correlated as a function of the significant independent variables. Data on the rate of transfer between beds or particles and a flowing fluid are needed in the design of many industrial devices used for extraction, adsorption, leaching, ion exchange and chromatography. Numerous studies for

packed beds have been carried out with the object of measuring mass-transfer coefficients and correlating the results under standard conditions, usually at 1 atm and 25°C. As far as we know, no data have been published on the mass-transfer coefficients under supercritical conditions. As several researchers pointed out,[10,11] under supercritical conditions we expect correlations for mass-transfer coefficients to differ from those for mass-transfer coefficients of solid-gas or solid-liquid systems under standard conditions.

In general, mass-transfer between a fluid and a packed bed of solid can be described by correlations of the following form by the similarity to the relationships obtained for heat transfer:

$$Sh = f(Re,Sc,Gr) \qquad (2\text{-}13)$$

where Sh, Re, Sc, and Gr are respectively the Sherwood number, Reynolds, Schmidt, and Grashof numbers for the mass-transfer. Such a relationship has been obtained theoretically by Eckert[49] from a consideration of the boundary conditions.

Below we describe several existing correlations, developed under non-supercritical conditions, which may serve as guides for the correlations to be developed in this work.

Natural Convection

Recently, Debenedetti and Reid[50] pointed out that, in the case of supercritical fluids, buoyant effects had to be considered because supercritical fluids showed extremely small kinematic viscosities as a result of their high densitites and low viscosities. The comparison of the properties of air, water, and mercury was given in Figure 2-8 to show the relative importance of buoyant forces

at constant Reynolds number. From the last column in Figure 2-8, we can find that the effect of buoyant forces is more than two orders of magnitude higher in supercritical fluid than in normal liquids.

For transfer under natural convection condition, where the Reynolds number is unimportant, general expression reduces to

$$Sh = g(Sc,Gr) \tag{2-14}$$

For large Schmidt number (usually liquid system) Karabeal et al.[51] proposed the following typical form of relationship for this natural convection condition by the use of asymptotic relations.

$$Sh = 0.46(GrSc)^{1/4} \tag{2-15}$$

for laminar natural convection

$$Sh = 0.112(GrSc)^{1/3} \tag{2-16}$$

for turbulent natural convection.

If natural convection is dominant, the correlations like those above are likely to be appropriate for modeling the mass-transfer coefficient data. Its main difference is that it is independent of Reynolds number Re.

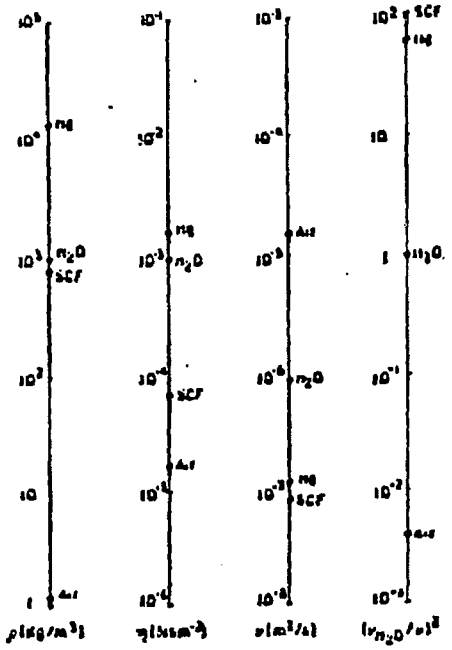

Figure 2-8: Comparison of physical properties of air, water, and mercury, and CO_2, showing relative importance of natural convection at constant Reynolds numbers: air, H_2O, Hg at 298°K and 1 bar, CO_2 at 310°K and 150 bar[50]

Forced Convection

Under forced convection conditions, where the Grashof number is unimportant, the general expression becomes

$$Sh = h(Re,Sc) \tag{2-17}$$

The most convenient method of correlating mass-transfer data under forced convection conditions is to plot the j_d factor as a function of Reynolds number as suggested by Colburn[5] and Chilton and Colburn[6] who, from theoretical consideration of flow and from dimensional analysis, defined j_d as follows:

$$j_d = \frac{Sh}{ReSc^{1/3}} = \frac{k_y M_{av}}{G}\left(\frac{\mu}{\rho D_v}\right)^{2/3} \tag{2-18}$$

In calculating the Schmidt number, $\mu/\rho D_v$, the viscosity and density of carbon dioxide will be used since the amount of naphthalene in carbon dioixde has a negligible effect on these properties.

The functional dependence of j_d on Reynolds number Re has been the subject of study by many investigators. A variety of equations have been proposed to represent their experimental data. Many of these correlations also employ the bed porosity ε as an additional correlating parameter. The porosity is the ratio of the void volume between pellets to the total bed volume. Two typical correlations for solid-gas and solid-liquid systems are as follows:

1. Solid - Gas System:[52]

$$\varepsilon j_d = 0.357\ Re^{-0.359} \qquad 3 < Re < 2000 \tag{2-19}$$

2. Solid-Liquid System:[8]

$$\epsilon j_d = 0.25\ Re^{-0.31} \qquad 55 < Re < 1500 \qquad (2\text{-}20)$$

$$\epsilon j_d = 1.09\ Re^{-2/3} \qquad 0.0016 < Re < 55 \qquad (2\text{-}21)$$

Other proposed correlations of mass-transfer data are shown in Rable 2-4.[51]

Combined Natural and Forced Convection

In the intermediate region where natural and forced convection happen simultaneously, neither the Reynolds number nor the Grashof number can be neglected. Garner and Grafton[53] suggested that the transfers due to the two processes are simply additive. Karabelas et al.[51] proposed the following correlations using an asymptotic method which are shown in Figure 2-9.

$$Sh = [\{0.46(GrSc)^{1/4}\}^6 + \{4.58\ pe^{1/3}\}^6]^{1/6} \qquad (2\text{-}22)$$

for 1 in, and 1/2 in, speheres ($GrSc < 1.31 \times 10^8$)

$$Sh = [\{0.112(GrSc)^{1/3}\}^2 + \{2.39\ Re^{0.56}Sc^{1/3}\}^2]^{1/2} \qquad (2.23)$$

For 3 in, sphere ($GrSc = 3.2 \times 10^9$)

Table 2-4: Correlations of mass-transfer data [51]

Reference	Type of packing	Correlation	Re	Sc
61	Spherical and cylindrical pellets	$j_d = 16{\cdot}8Re^{-1}$	< 40	0·61–0·62
		$j_d = 0{\cdot}989Re^{-0.41}$	> 350	
62	Same as above	$j_d = 1{\cdot}82Re^{-0.51}$	< 350	~ 0·615
63	Granular solid	$StSc^{0.4} = 0{\cdot}45Re^{-0.28}$	< 10	~ 1000
		$StSc^{0.4} = 0{\cdot}20Re^{-0.36}$	> 50	
64	Spheres and cylinders	$j_d = 1{\cdot}251Re_m^{-0.41}$	$Re_m \geq 620$	~ 0·61
		$j_d = 2{\cdot}44Re_m^{-0.66}$	$Re_m < 620$	
65	Spherical and flake shaped particles	$j_d = 1{\cdot}625Re^{-0.643}$	< 120	1200–1500
		$j_d = 0{\cdot}687Re^{-0.422}$	> 120	
66	Porous spherical particles soaked in an aqueous solution	$\log j_d = 0{\cdot}7683 - 0{\cdot}915 \log Re + 0{\cdot}0817 [\log Re]^2$	0–10,000	776 and 865
67	Pellets of succinic and salicylic acids	$StSc^{0.56} = 1{\cdot}97\left[\frac{Re}{\epsilon}\right]^{-0.613}$	$\frac{Re}{\epsilon} < 200$	150–13,000
		$StSc^{0.56} = 0{\cdot}29\left[\frac{Re}{\epsilon}\right]^{-0.359}$	$\frac{Re}{\epsilon} > 200$	
68	Various particle geometries	$j_d = \frac{150(1-\epsilon)}{6\epsilon} Re^{-1}Sc^{-1/3} + \frac{1{\cdot}75}{6\epsilon} Sc^{-1/3}$	wide range	wide range
69	Spheres	$j_d = 1{\cdot}46\left[\frac{6G}{a\mu}\right]^{-0.41}(1-\epsilon)^{0.4}$	$\frac{6G}{a\mu} > 100$	wide range
		$j_d = 17\left[\frac{6G}{a\mu}\right]^{-1}(1-\epsilon)^{0.4}$	$\frac{6G}{a\mu} < 10$	
70	Porous spheres	$j_d = 10Re^{-1}$	< 50	low
		$j_d = 1{\cdot}30Re^{-0.5}$	> 150	
71	Benzoic acid granules	$j_d = 1{\cdot}48Re^{-0.51}$	1–70	~ 1000
72	Various particle types	$j_d = 5{\cdot}7\left[\frac{Re}{1-\epsilon}\right]^{-0.78}$	$1 < \frac{Re}{1-\epsilon} < 30$	0·6–10,000
		$j_d = 1{\cdot}77\left[\frac{Re}{1-\epsilon}\right]^{-0.44}$	$30 < \frac{Re}{1-\epsilon} < 10^4$	
73	Spherical particles	$j_d = 0{\cdot}667Re^{-0.56}$	20–200	
74	Porous spheres	$j_d = \frac{0{\cdot}725}{Re^{0.41} - 1{\cdot}5}$	13–2136	0·606
7	Fixed and fluidized beds of spheres	$\epsilon j_d = 0{\cdot}010 + \frac{0{\cdot}863}{Re^{0.56} - 0{\cdot}483}$	> 1	wide range
75	Fixed and fluidized beds of particles with various geometries	$\frac{\epsilon j_d}{f} = \frac{0{\cdot}30}{Re_m^{0.50} - 1{\cdot}90}$	$Re_m > 50$	wide range
76	Spherical particles	$StSc^{0.56} = 2{\cdot}40\left[\frac{Re}{\epsilon}\right]^{-0.66}$	$0{\cdot}08 < \frac{Re}{\epsilon} < 125$	~ 1000
		$StSc^{0.56} = 0{\cdot}442\left[\frac{Re}{\epsilon}\right]^{-0.31}$	$125 < \frac{Re}{\epsilon} < 5000$	
77	Porous spherical and cylindrical particles	$j_d = 2{\cdot}25\left[\frac{Gd}{\mu}\frac{1}{1-\epsilon}\right]^{-0.61}$	wide range	0·60

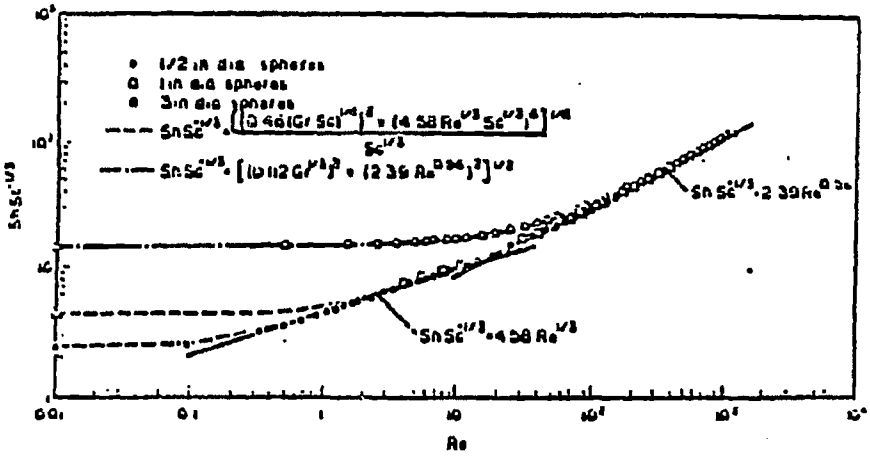

Figure 2-9: Asymptotic correlations for the combined natural and forced convection[51]

2.5 Experimental

The schematic diagram of the experimental apparatus used in this study is shown in Figure 2-10. Liquid carbon dioxide is pumped into the system via a high-pressure Milton-Roy liquid pump. Pressure is controlled by using a back pressure regulator and pressure fluctuation is dampened with an on-line surge tank. The system consists of a preheater which allows the solvent to reach the desired temperature and the extraction vessel 171 cm^3 in volume, 14.6 cm in length and 3.87 in diameter. The extraction vessel is packed with naphthalene pellets which have been made from pure naphthalene using a die. The height of the packing in the bed can be changed by using inert packing at the bottom and the top of the bed. The inert packing material being used is glass beads with size similar to that of the pellets. Another advantage in using the inert pellets is to get rid of end effects in the packed bed being used as the extractor. Pressure at the inlet of extractor is measured using a pressure transducer. The temperature of the extractor is measured at the inlet.

The fluid mixture coming out of the extractor is depressurized to atmospheric pressure by passing it through a heated metering valve and a back pressure regulator. The instantaneous flow rate of the gas leaving the extractor is measured using a rotameter and the total amount of gas flow is measured with a calibrated wet-test meter.

The mass of precipitated solid is found as described below. With this value and total amount of gas flow through wet-test meter, the mole fraction of solids in the supercritical fluid can be readily determined. The temperature and pressure in wet-test meter are also measured.

The sample collectors are high pressure bombs which are kept at room temperature by two 200 watt resistance heaters. Each vessel contains toluene

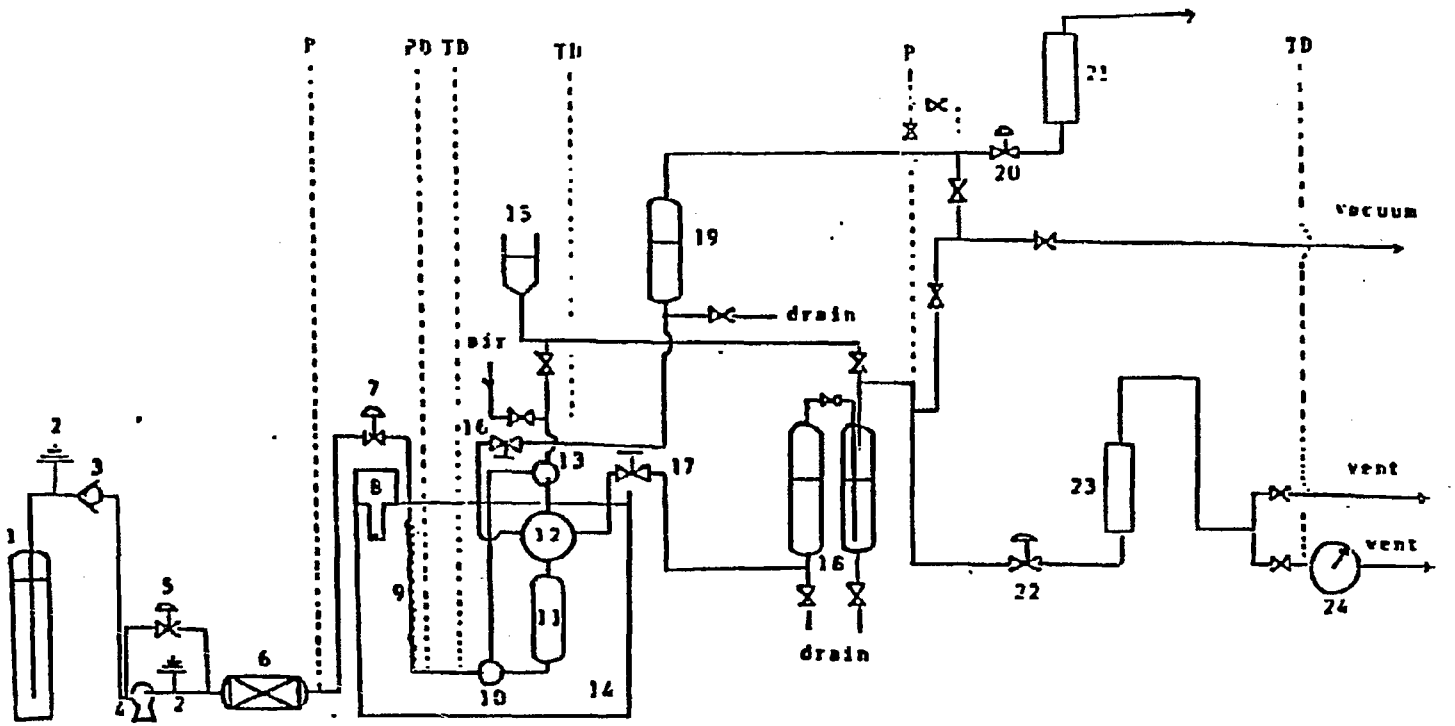

1. Cylinder
2. Relief valve
3. Check valve
4. Liquid pump
5. Back pressure regulator
6. Surge tank
7. Pressure regulator
8. Temperature controller
9. Preheater
10. Three-way valve
11. Extractor
12. Four-way valve
13. Three-way valve
14. Water bath
15. Solvent tank
16. Metering valve
17. Metering valve
18. Sample tanks
19. Solid trap
20. Back pressure regulator
21. Rotameter
22. Back pressure regulator
23. Rotameter
24. Wet test meter

P: Pressure gauge
PD: Pressure transmitter to Data logger
TD: Thermocouple to Data logger

Figure 2-10: Schematic diagram of the experimental apparatus of SCFE

which will help dissolve the extract (naphthalene) from the carbon dioxide. These vessels are operated at 300 to 400 psi where the solubility of the solid in the carbon dioxide is at a minimum. The second vessel is redundant and is used to guarantee that all of the extract is collected and to reduce entrainment losses. No naphthalene was found in these vessels during current experiments. To determine the amount of extract collected, the amount of toluene (with dissolved extract) is weighed. A sample of the toluene-extract solution is then injected into a gas chromatograph to determine what portion of the solution is extract. Finally, the bypass, from valve 12 to 16, is designed to insure steady-state flow through the extraction vessel 11.

The whole apparatus is rated for a pressure of 5000 psi. All measured temperatures and pressures are recorded on a data logger at regular time intervals. The parameters that are being studied are:

- Effect of flow rate on solubility of naphthalene in carbon dioxide at different pressures and temperatures.
- Effect of bed height on the mass-transfer coefficient under supercritical conditions.
- Effect of flow rate on the mass-transfer coefficient under supercritical conditions.
- Effect of pressure on the mass-transfer coefficient under supercritical conditions.

The experimental conditions are as follows:

System: Naphthalene - Carbon Dioxide

Pellet Characteristics:

Material: Naphthalene

Shape: Cylindrical

Size: Length (mm) = 4.76

Diameter (mm) = 4.76

Height of Bed (mm): 4.76 - 19.04

Temperature of Bed (^{o}K): 308, 318, 328

Pressure (psi): 1470, 2205, 2940, 3675

Flow Rates (STD. liter/min at 0^{o}C and 1 atm): 4 - 30

Reynolds Number: $10 < Re < 250$

Schmidt Number: $5 < Sc < 12$

Grashof Number: $1.69 \times 10^{6} < Gr < 2.13 \times 10^{7}$

2.6 Plans

This work is divided into two major parts. The first part is to measure mass-transfer coefficients, while the second one is concerned with establishing the mass-transfer correlations under supercritical conditions.

Mass-transfer coefficients in packed beds under standard conditions have been measured using various flow models. However, no study has yet been carried out to estimate the mass-transfer coefficient under supercritical conditions and no mass-transfer correlations under these conditions have been developed.

For this fundamental mass-transfer study under supercritical conditions, naphthalene-CO_2 systems have been chosen due to convenience of getting the values of transport properties such as binary diffusion coefficient, viscosity and density of carbon dioixde from the literature. Experiments are being carried out to investigate the effect of the flow rate of CO_2 on solubility of naphthalene in CO_2.

The effect of flow rate on CO_2, temperature, and pressure on mass-transfer coefficients will be determined using the plug flow model and cell model. Then, these mass-transfer coefficient data will be used to developed mass-transfer correlations analogous to those shown in the previous section which would be useful in designing separation units. Finally, these correlations for solid-supercritical fluid will be compared with mass-transfer correlations for solid-gas and/or solid-liquid systems, depending upon three different flow conditions, respectively (natural, forced, and combined natural and forced convection).

Results

Work for current period (October 1 - December 31, 1987).

Two layers of naphthalene pellets (as compared to the single layer used previously) were used to get mass transfer coefficients in a packed bed. We operated our system continuously for 2 to 4 minutes at 35°C and 100 atm or 150 atm for several flow rates of carbon dioxide. Mass transfer coefficients were calculated by both the ideal model and the cell model. Those data are shown in Tables 2-5 and 2-6 for 100 atm and 150 atm, respectively. Their comparison were shown in Figures 2-11 and 2-12 for the ideal model and Figures 2-13 and 2-14 for the cell model.

We found the relationship between mole fraction y and bed height L_T with k_y values obtained for the given mass velocity G. The design curves at 100 atm and 150 atm, respectively, were given in Figures 2-15 and 2-18 for two models.

More data, especially in low flow rate, are needed to determine the true correlationship between dimensionless groups (Sh, Sc, Re, Gr). The different experiment conditions (different temperatures and pressures) will also be studied in the following quarter.

Table 2.5

Data of Mass Transfer Coefficients and Dimensionless Group at 35°C and 100.0 atm (Yeq = 0.01026)

Run No	Velocity l/min	Ynap Mol-frac	G gr/cm2 sec	Ky Id	Ky Cell	Re	Jd Id	Jd Cell
1	22.0505	0.58448E-02	0.06011	0.1855E-03	0.2148E-03	46.37	0.5172	0.5990
7	19.8648	0.51352E-02	0.05410	0.1440E-03	0.1625E-03	40.77	0.4463	0.5034
5	18.1768	0.54016E-02	0.04952	0.1512E-03	0.1721E-03	36.14	0.5117	0.5827
6	17.6187	0.54295E-02	0.04800	0.1315E-03	0.1499E-03	37.15	0.4592	0.5234
4	16.3814	0.56184E-02	0.04464	0.1311E-03	0.1505E-03	34.23	0.4922	0.5650
2	14.9926	0.54120E-02	0.04085	0.1209E-03	0.1377E-03	30.33	0.4961	0.5651
9	14.3153	0.53882E-02	0.03900	0.1667E-03	0.1897E-03	28.63	0.7166	0.8156
3	12.7412	0.64571E-02	0.03477	0.1217E-03	0.1447E-03	27.31	0.5868	0.6977
11	8.4220	0.70564E-02	0.02300	0.1670E-03	0.2048E-03	16.15	1.2173	1.4924
10	6.8277	0.70741E-02	0.01865	0.1273E-03	0.1562E-03	13.57	1.1442	1.4042
8	6.1236	0.87563E-02	0.01677	0.1181E-03	0.1661E-03	12.90	1.1804	1.6608
12	2.1012	0.97587E-02	0.00576	0.8891E-04	0.1541E-03	4.49	2.5869	4.4832
13	1.5335	0.92325E-02	0.00420	0.4823E-04	0.7286E-04	3.31	1.9243	2.9069

Run	Sh^{id}	Sh^{cl}	Sc	Gr	ScGr	$ky^{id} \cdot a_s$	$ky^{cl} \cdot a_s$
1	46.6792	54.0575	7.3730	0.28986925E+07	0.21371962E+08	0.1282E-02	0.1485E-02
7	35.4234	39.9595	7.3806	0.28302785E+07	0.20889188E+08	0.9732E-03	0.1098E-02
5	35.9996	40.9925	7.3777	0.25270723E+07	0.18644090E+08	0.9903E-03	0.1128E-02
6	33.2051	37.8488	7.3774	0.30075538E+07	0.22188050E+08	0.9123E-03	0.1040E-02
4	32.8025	37.6536	7.3754	0.28909005E+07	0.21321564E+08	0.9014E-03	0.1035E-02
2	29.2927	33.3680	7.3776	0.26608145E+07	0.19630502E+08	0.8051E-03	0.9171E-03
9	39.9352	45.4518	7.3779	0.25733263E+07	0.18985708E+08	0.7726E-03	0.8793E-03
3	31.1802	37.0766	7.3664	0.29366388E+07	0.21632376E+08	0.8566E-03	0.1019E-02
11	38.2283	46.8698	7.3599	0.20074770E+07	0.14774869E+08	0.7434E-03	0.9115E-03
10	30.2043	37.0686	7.3597	0.22345540E+07	0.16445714E+08	0.5841E-03	0.7168E-03
8	29.6056	41.6547	7.3416	0.23171540E+07	0.17011716E+08	0.8140E-03	0.1145E-02
12	22.5446	39.0702	7.3309	0.21963490E+07	0.16101164E+08	0.4342E-03	0.7525E-03
13	12.3895	18.7161	7.3365	0.23927175E+07	0.17554236E+08	0.2384E-03	0.3602E-03

Table 2.6

Data of Mass Transfer Coefficients and Dimensionless Group
at 35°C and 150.0 atm (Yeq = 0.01470)

Run No	Velocity l/min	Ynap Mol-frac	G gr/cm2 sec	ky Id	ky Cell	Re	Jd Id	Jd Cell
5	26.6223	0.44432E-02	0.09431	0.1546E-03	0.1647E-03	53.67	0.3273	0.3485
7	23.9874	0.55740E-02	0.08512	0.1820E-03	0.1978E-03	48.88	0.4269	0.4639
18	18.3075	0.52359E-02	0.06493	0.1436E-03	0.1551E-03	35.15	0.4416	0.4769
11	17.6380	0.64759E-02	0.06267	0.1536E-03	0.1700E-03	37.11	0.4892	0.5415
4	16.3566	0.58091E-02	0.05806	0.1255E-03	0.1370E-03	34.10	0.4315	0.4711
2	16.2936	0.71412E-02	0.05795	0.1899E-03	0.2134E-03	31.64	0.6542	0.7351
9	13.4366	0.59950E-02	0.04771	0.1101E-03	0.1207E-03	27.69	0.4607	0.5048
12	12.3405	0.61523E-02	0.04383	0.1028E-03	0.1130E-03	25.67	0.4683	0.5148
3	12.3186	0.63892E-02	0.04376	0.1130E-03	0.1248E-03	25.03	0.5153	0.5694
13	10.5981	0.72935E-02	0.03770	0.1107E-03	0.1248E-03	22.18	0.5859	0.6606
8	10.0817	0.72866E-02	0.03586	0.9879E-04	0.1114E-03	21.78	0.5498	0.6199
6	9.8164	0.76034E-02	0.03494	0.1060E-03	0.1204E-03	20.84	0.6056	0.6881
10	9.0405	0.75917E-02	0.03217	0.9567E-04	0.1087E-03	19.37	0.5935	0.6741
19	8.8536	0.79056E-02	0.03152	0.1039E-03	0.1189E-03	18.57	0.6577	0.7530
16	8.7261	0.79176E-02	0.03107	0.1047E-03	0.1199E-03	18.11	0.6724	0.7701
17	7.2724	0.78855E-02	0.02589	0.9149E-04	0.1047E-03	14.67	0.7053	0.8071
14	4.5753	0.70247E-02	0.01627	0.4255E-04	0.4768E-04	9.89	0.5221	0.5850
1	4.3600	0.13457E-01	0.01565	0.2148E-03	0.3358E-03	8.05	2.7395	4.2818
20	4.1370	0.81051E-02	0.01473	0.4813E-04	0.5540E-04	8.89	0.6520	0.7504
15	1.5504	0.12727E-01	0.00556	0.4435E-04	0.6354E-04	3.39	1.5920	2.2810

Run	Sh^{id}	Sh^{cl}	Sc	Gr	ScGr	$ky^{id} \cdot a_s$	$ky^{cl} \cdot a_s$
5	37.3380	39.7583	9.5990	0.33320208E+07	0.31984204E+08	0.9195E-03	0.9791E-03
7	44.3216	48.1716	9.5832	0.32752748E+07	0.31387612E+08	0.1088E-02	0.1183E-02
18	32.9797	35.6162	9.5879	0.27809570E+07	0.26663630E+08	0.8136E-03	0.8786E-03
11	38.5464	42.6686	9.5706	0.34595480E+07	0.33109872E+08	0.9458E-03	0.1047E-02
4	31.2476	34.1179	9.5799	0.34687270E+07	0.33230090E+08	0.7654E-03	0.8357E-03
2	43.9307	49.3577	9.5613	0.26353298E+07	0.25197106E+08	0.1086E-02	0.1220E-02
9	27.0893	29.6878	9.5773	0.33237513E+07	0.31832586E+08	0.6630E-03	0.7265E-03
12	25.5254	28.0638	9.5751	0.33938610E+07	0.32496578E+08	0.6244E-03	0.6865E-03
3	27.3908	30.2640	9.5718	0.31297495E+07	0.29957310E+08	0.6714E-03	0.7418E-03
13	27.5812	31.1000	9.5591	0.32770913E+07	0.31326190E+08	0.6753E-03	0.7615E-03
8	25.4197	28.6581	9.5592	0.36060913E+07	0.34471500E+08	0.6215E-03	0.7006E-03
6	26.7858	30.4324	9.5548	0.33697098E+07	0.32196952E+08	0.6555E-03	0.7447E-03
10	24.3960	27.7092	9.5550	0.34649610E+07	0.33107624E+08	0.5968E-03	0.6779E-03
19	25.9055	29.6599	9.5506	0.31985840E+07	0.30548370E+08	0.6347E-03	0.7267E-03
16	25.8394	29.5935	9.5504	0.30997643E+07	0.29604058E+08	0.6335E-03	0.7255E-03
17	21.9516	25.1198	9.5509	0.28500345E+07	0.27220314E+08	0.5399E-03	0.6178E-03
14	10.9548	12.2749	9.5629	0.36513660E+07	0.34917660E+08	0.2676E-03	0.2998E-03
1	46.6477	72.9099	9.4732	0.15894558E+07	0.15057274E+08	0.1149E-02	0.1796E-02
20	12.2954	14.1519	9.5478	0.34074460E+07	0.32533626E+08	0.3007E-03	0.3461E-03
15	11.4281	16.3749	9.4834	0.27742030E+07	0.26308832E+08	0.2799E-03	0.4011E-03

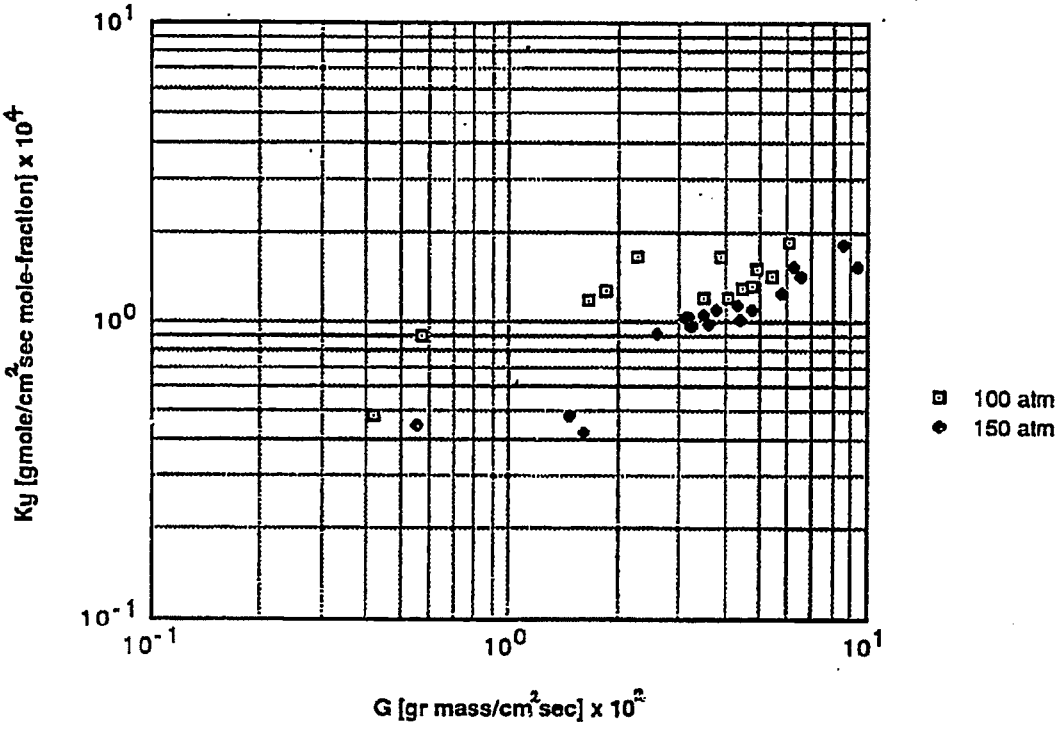

Figure 2-11: **Correlation between Kg and G at 35 C by the ideal model**

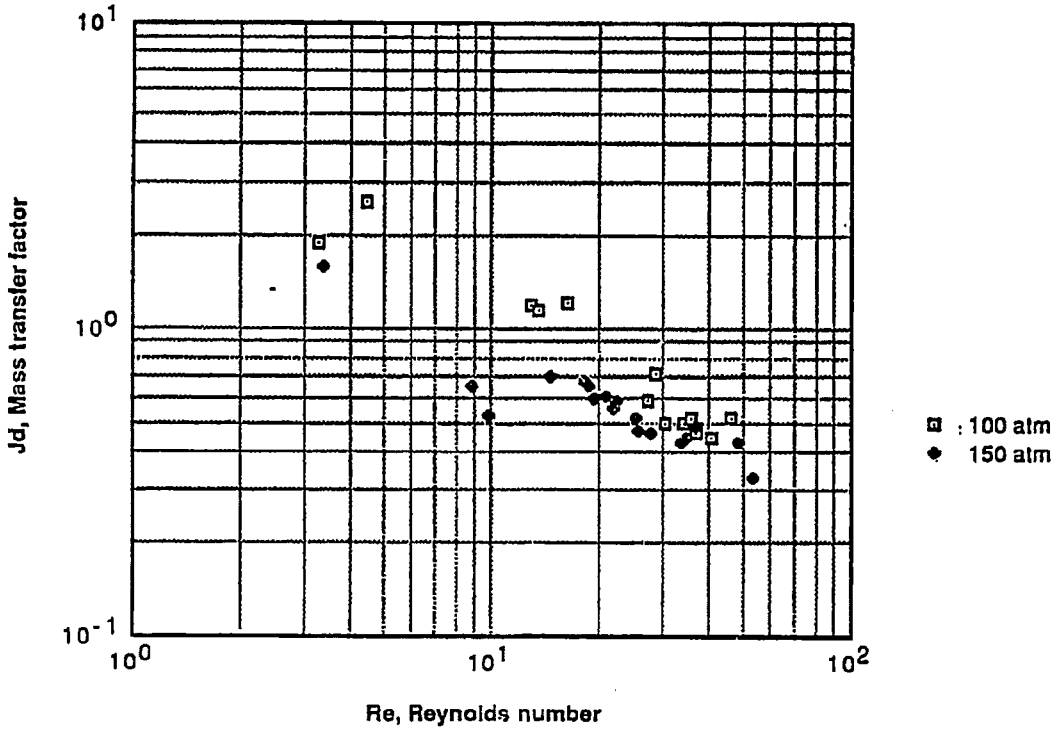

Figure 2-12: **Correlation between Jd and Re at 35 C by the ideal model**

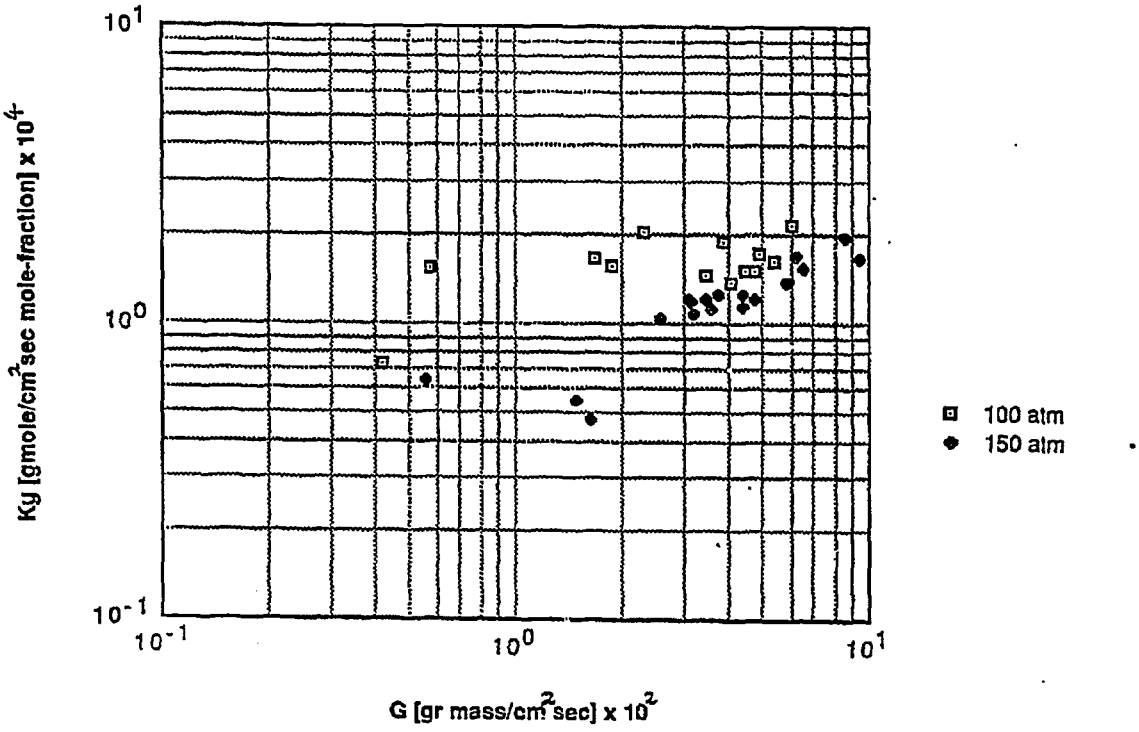

Figure 2-13: **Correlation between Kg and G at 35 C by the cell model**

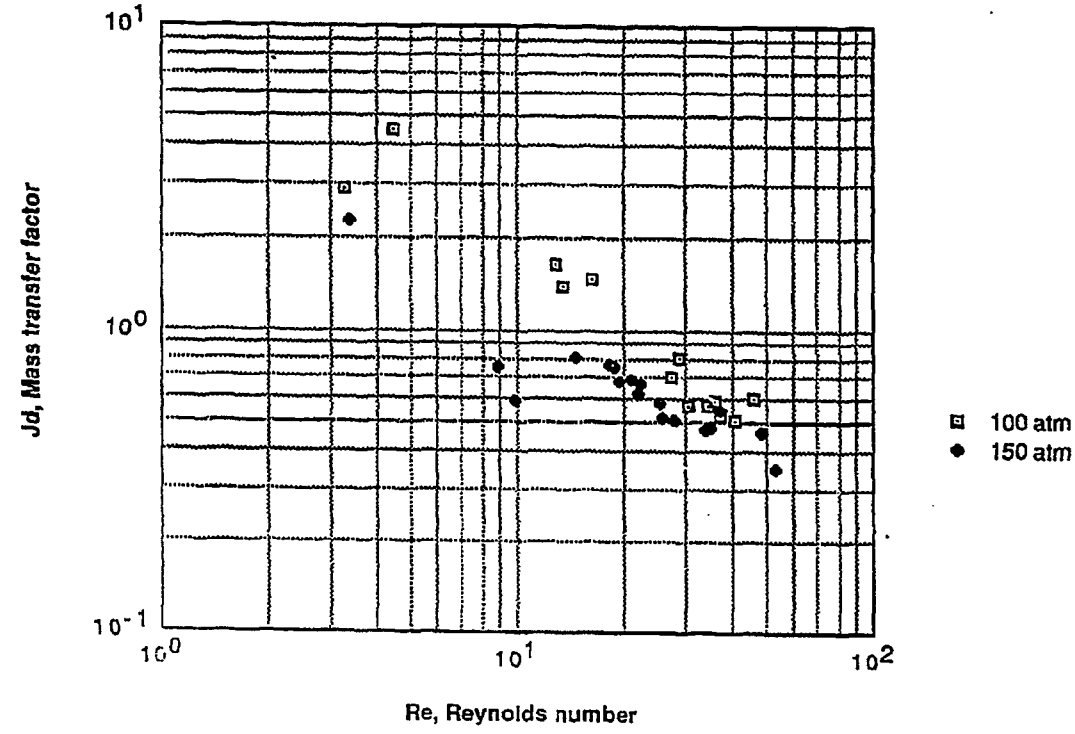

Figure 2-14: **Correlation between Jd and Re at 35 C by the cell model**

Figure 2-15: Design Curve at 35 C and 100 atm by the Ideal Model

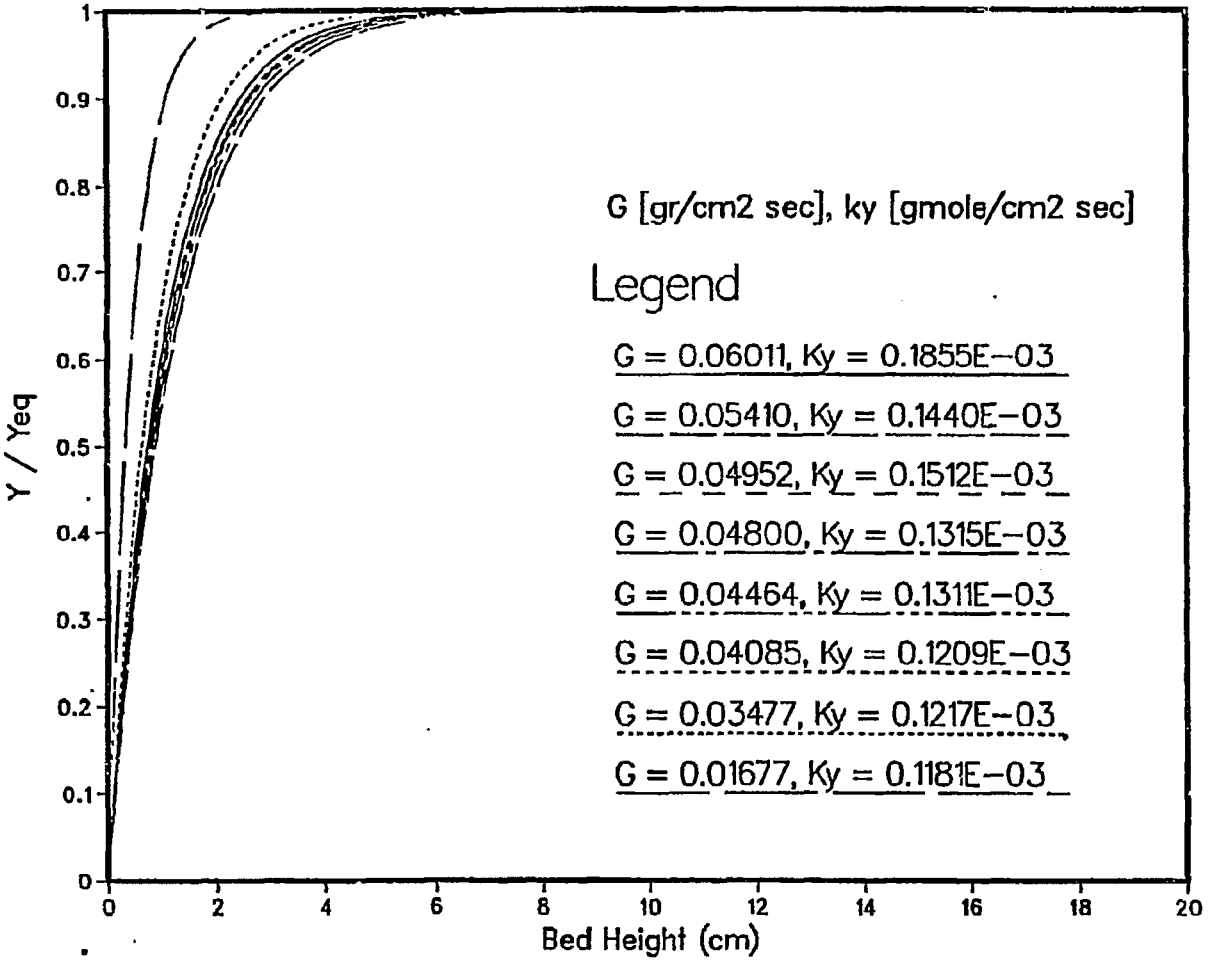

Figure 2-16: Design Curve at 35 C and 100 atm by the Cell Model

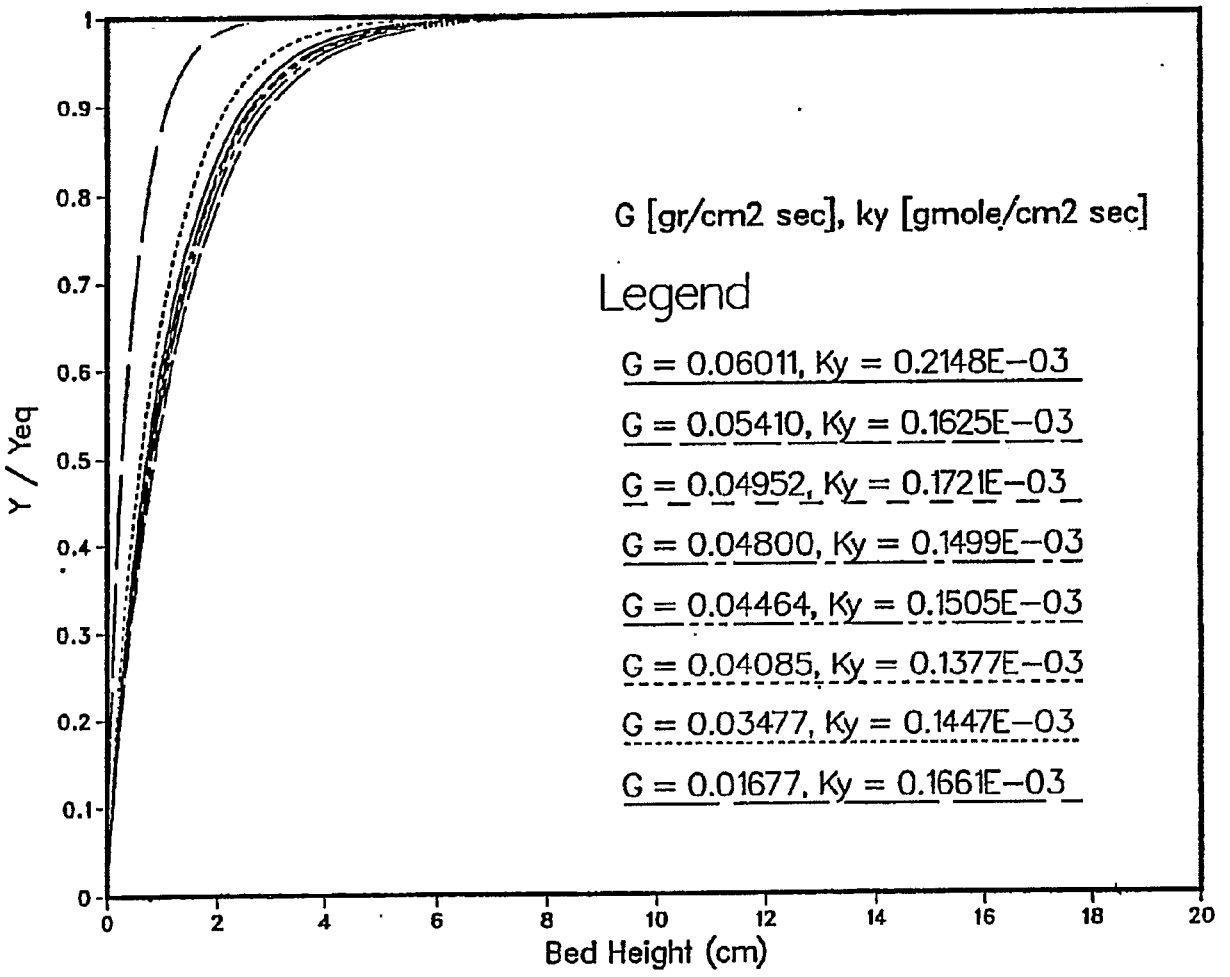

Figure 2-17: Design Curve at 35 C and 150 atm by the Ideal Model

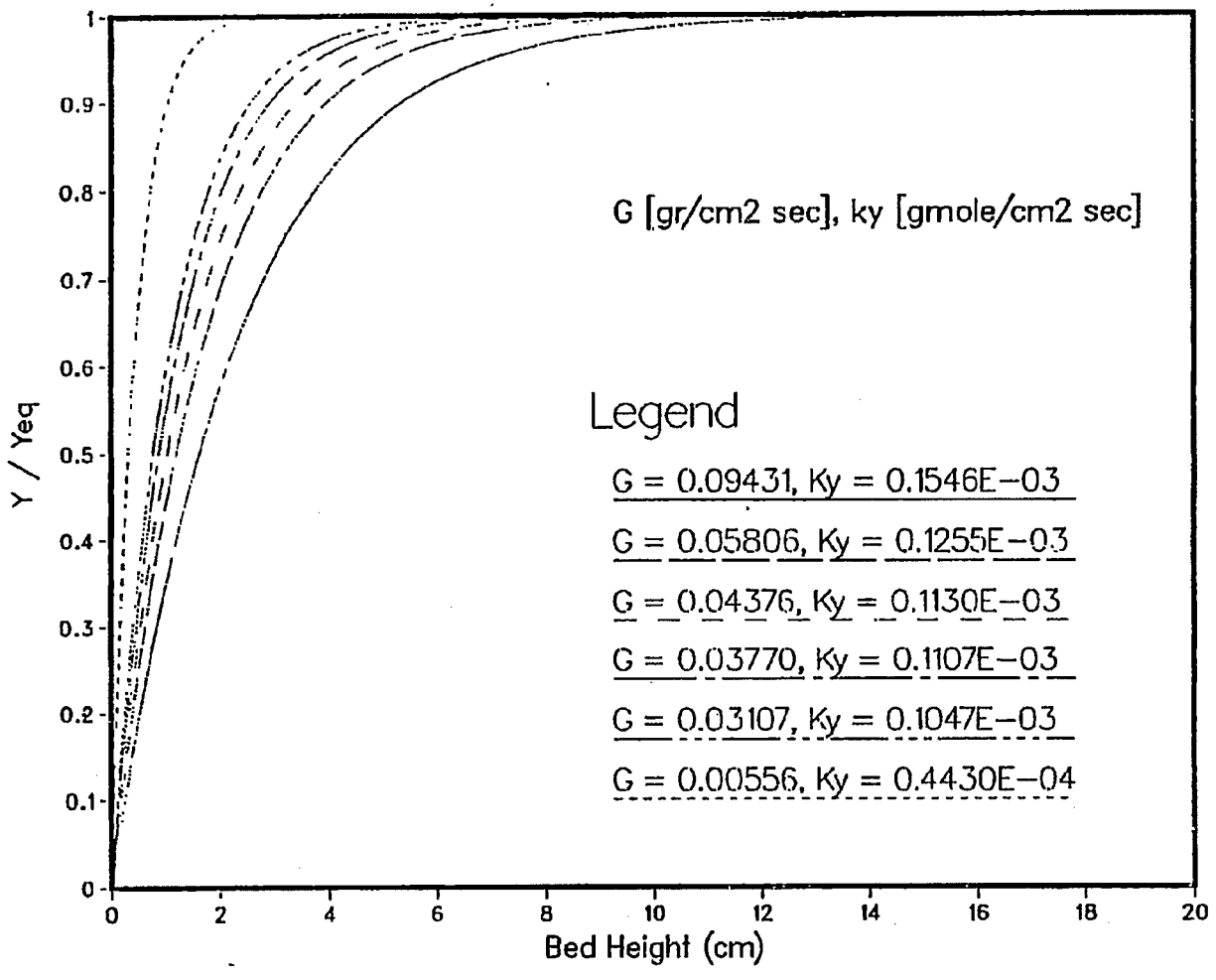

Figure 2-18: Design Curve at 35 C and 150 atm by the Cell Model

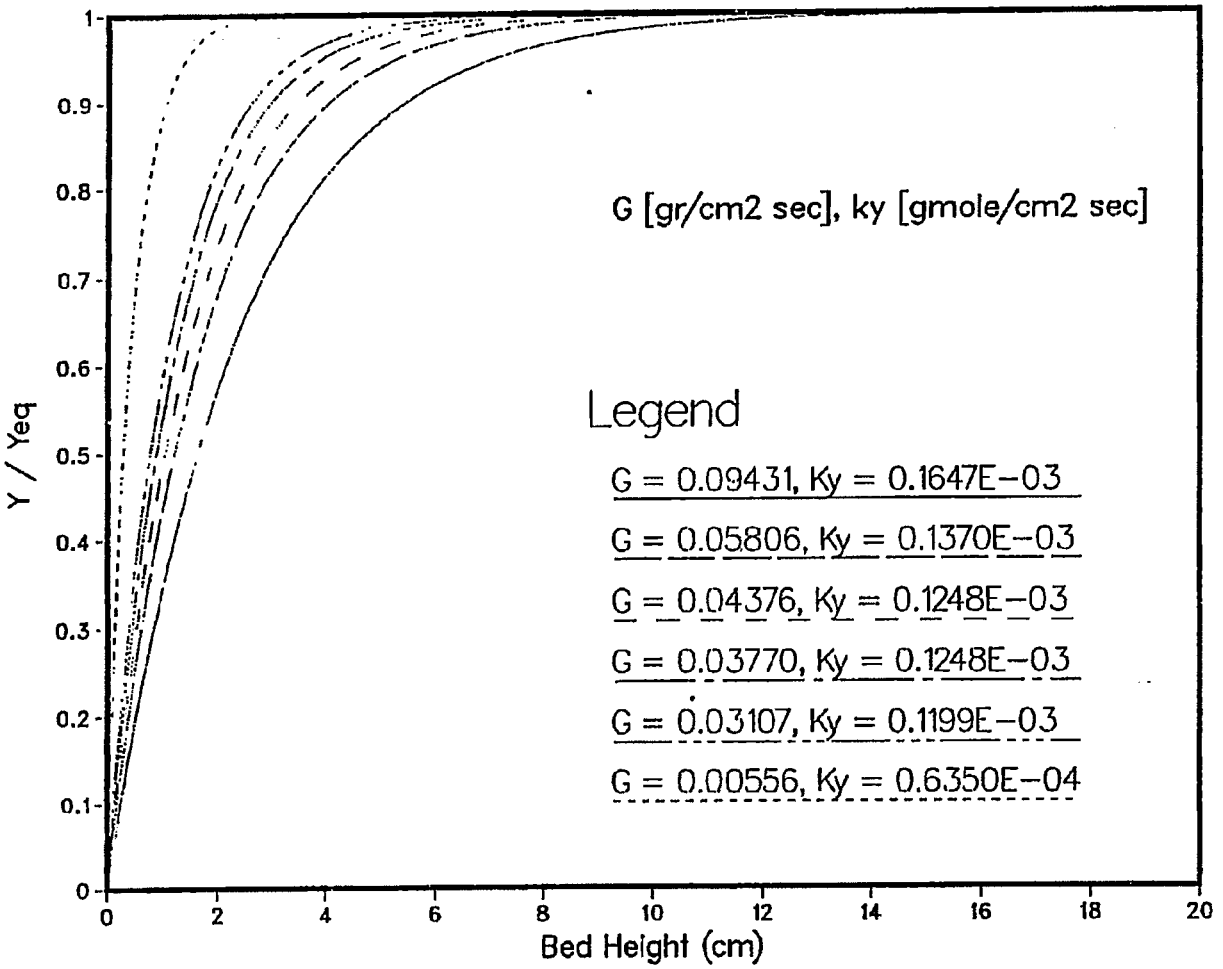

NOMENCLATURE

a	:	System parameter in Peng-Robinson equation of state
a_S	:	Surface area of pellets per unit volume of extractor [cm^2/cm^3]
A_p	:	Surface area of single particle [cm^2]
A_T	:	Total surface area of pellets in extractor [cm^2]
b	:	System parameter in Peng-Robinson equation of state
C	:	Concentration of solute [$gmole/cm^3$]
d_p	:	Diameter of sphere possessing the same surface area as a piece of packing [cm]
D_v	:	Molecular diffusivity [cm^2/sec]
E_a	:	Axial dispersion coefficient [cm^2/sec]
E_r	:	Radial dispersion coefficient [cm^2/sec]
f_i^s	:	Fugacity of component i in solid phase [atm]
f_i^v	:	Fugacity of component i in vapor phase [atm]
g	:	Gravitational acceleration [cm/s
G	:	Mass velocity [g/cm^2sec]
$\bar{G}_{My}$	:	Average molal mass velocity [$gmole/cm^2sec$]
G_{My}	:	Molal mass velocity [$gmole/cm^2sec$]
Gr	:	Grashof number = $d^3g\rho\Delta\rho/\mu^2$
j_d	:	Mass transfer factor = $ShRe^{-1}Sc^{-1/3}$
k_c	:	Mass transfer coefficient = k_yC [cm/sec]
k_{ij}	:	Binary interaction parameter
k_y	:	Mass transfer coefficient [$gmole/cm^2sec$ mole-fraction]
k_y^{id}	:	Mass transfer coefficient by the ideal plug flow model
k_y^{cl}	:	Mass transfer coefficient by the cell model
L_T	:	Total height of bed [cm]

M_{av}	:	Average molecular weight [g/gmole]
n	:	Number of perfect mixers
N_A	:	Molal flux of solute [gmole/cm^{2}sec]
P	:	Total pressure [atm]
P_c	:	Critical pressure [atm]
Pe	:	Peclet number = $u_s d_p/D_v$
$P_{e,a}$	:	Axial peclet number = ud_p/E_a
P_I^s	:	Saturation (Vapor) pressure of pure solid [atm]
R	:	Gas constant = 0.08205 [atm liter/gmole ^oK]
Re	:	Reynolds number = $\rho d_p u_s/\mu$
S	:	Cross section area of packed bed [cm^2]
Sc	:	Schmidt number = $\mu/\rho D_v$
Sh	:	Sherwood number = $k_c d_p/D_v$
Sh^{id}	:	Sherwood number by the ideal plug flow model
Sh^{Cl}	:	Sherwood number by the cell model
T	:	Absolute temperature
T_c	:	Critical temperature [^oK]
T_r	:	Reduced temperature
T_ε	:	Tortuosity of bed
u	:	Interstitial velocity [cm/sec]
u_s	:	Superficial velocity [cm/sec]
V_T	:	Total molal flow rate [gmole/sec]
V'	:	Molal flow rate of inert component [gmole/sec]
y_A	:	Mole fraction of component A
y_A^*	:	Equilibrium mole fraction of component of A
y_i	:	Mole fraction of component A in stream outgoing from ith cell
Z	:	Compressibility factor

Greek Letters

ε	:	Void fraction
Φ_{iv}	:	Fugacity coefficient of component i in vapor phase
Φ_{is}^{s}	:	Fugacity coefficient of component i in solid phase at saturaction pressure P_i^s
γ_i^{∞}	:	Activity coefficient at infinite dilution
μ	:	Viscosity [g/cm sec]
ρ	:	Density [g/cm^3]

BIBLIOGRAPHY

1. Chang, H. and Morrell, D.G., "Solubilities of Methoxy-1-Tetralone and Methyl Nitrobenzoate Isomers and their Mixtures in Supercritical Carbon Dioxid," J. Chem. Eng. Data, Vol. 30, 1985, pp.74.

2. Irani, C.A. and Funk, E.W., Separation Using Supercritical Gases, CRC Hand Book, CRC Press, Boca Raton, FL, 1977, pp. 171, Ch. Part A.

3. Paul, P.F.M. and Wise, W.S., The Properties of Gases Extraction, Mills and Boom Ltd., London, 1971.

4. Sirtl, W., "Examples of Cost Determinations," High Pressure Extraction Symposium, NOVA-WERKE AG. Effretikon, Switzerland, August 1979.

5. Colburn, A.P., "A Method of Correlating Forced Convection Heat Transfer Data and a Comparison with Fluid Friction," AIChE J., Vol. 29, 1933, pp. 174.

6. Chilton, T.H. and Colburn, A.P., "Mass-Transfer (Absorption) Coefficients (Prediction from Data on Heat Transfer and Fluid Friction)," Ind. Eng. Chem., Vol. 26, 1934, pp. 1183.

7. Gupta, A.S. and Thodos, G., "Mass and Heat Transfer in the Flow of Fluids through Fixed and Fluidized Beds of Spherical Particles," AIChE J., Vol. 8, 1962, pp. 608.

8. Wilson, E.J. and Geankoplis, C.J., "Liquid Mass-Transfer at Very Low Reynolds Numbers in Packed Beds," Ind. Eng. Chem. Fund., Vol. 5, 1966, pp. 9.

9. Storck, A. and Coeuret, F., "Mass-Transfer Between a Flowing Liquid and a Wall or an Immersed Surface in Fixed and Fluidized Beds," Chem. Eng. J., Vol. 20, 1980, pp. 149.

10. Pfeffer, R., "Heat and Mass Transfer in Multiparticle Systems," Ind. Eng. Chem. Fund., Vol. 3, 1964, pp. 380.

11. Bradshaw, R.D. and Bennett, C.O., "Fluid-Particle Mass Transfer in a Packed Bed," AIChE J., Vol. 7, 1961, pp. 48.

12. Hannay, J.B., "On the Solubility of Solids in Gases," Proc. Roy. Soc. (London), Vol. 30, 1880, pp. 484.

13. Hannay, J.B. and Hogarth, J., "On the Solubility of Solids in Gases," Proc. Roy. Soc. (London), Vol. 29, 1879, pp. 324.

14. Hannay, J.B. and Hogarth, J., "On the Solubility of Solids in Gases," Proc. Roy. Soc. (London), Vol. 30, 1880, pp. 178.

15. Buchner, E.H., "Flussige Kohlensaure als Losungsmittel," Z. Physik. Chem., Vol. 54, 1906, pp.665.

16. Centnerszwer, M., "Uber Kritische Temperaturen der Losungen," Z. Physik. Chem., Vol. 46, 1903, pp. 427.

17. Sage, B.H., Webster, D.C. and Lacey, W.N., "Phase Equilibria in Hydrocarbon Systems: XVI. Solubility of Methane in Four Light Hydrocarbons," Ind. Eng. Chem., Vol. 28, 1936, pp. 1045.

18. Kay, W.B., "Liquid-Vapor Phase Equilibrium Relations in the Ethane-n-Heptane System," Ind. Eng. Chem., Vol. 30, 1938, pp. 459.

19. Messmore, H.E., U.S. Pat. 2,420,185, 1943.

20. Maddocks, R.R. and Gibson, "Supercriticle Extraction of Coal," J. Chem. Eng. Progr., Vol. 73, 1977, pp. 59.

21. Tugrul, T. and Oclay, A., "Supercritical Gas Extraction of Two Lignites," Fuel, Vol. 57, 1978, pp. 415.

22. Bartle, K.D. et al., "Chemical Nature of a Supercritical-Gas Extract of Coal at 350°C," Fuel, Vol. 54, 1975, pp. 227.

23. Barton, P. and Fenske, M.R., "Hydrocarbon Extraction of Saline Water," Ind. Eng. Chem. Process Des., Vol. 9, 1970, pp. 18.

24. Hubert, P. and Vitzhum, O., "Fluid Extraction of Hops, Spices and Tobacco with Supercritical Gases," Agnew Chem. Inc., Vol. 17, 1978, pp. 710, England.

25. Modell, M., deFelippi, R.P. and Krukonis, V., "Regeneration of Activated Carbon with Supercritical Carbon Dioxide," Am. Chem. Soc. Meet., Miami, September 1978.

26. Modell, M. et al., "Supercritical Fluid Regeneration of Activated Carbon," 87th Nat. Meet. Am. Inst. Chem. Eng., 1979.

27. Diepen, G.A.M. and Scheffer, F.E.C., "The Solubility of Naphthalene in Supercritical Ethylene II," J. Phys. Chem., Vol. 57, 1953, pp. 575.

28. Tsekhanskaya, Yu., V., Iomtev, M.B. and Mushkina, E.V., "Solubility of Naphthalene in Ethylene and Carbon Dioxide under Pressure," Russ. J. Phys. Chem., Vol. 38, 1964, pp. 1173.

29. Modell, M. et al., ".", 72nd AIChE J. Annual Meeting, San Francisco, CA, Nov., 1979.

30. Mackay, M.E. and Paulaitis, M.E., "Solid Solubilities of Heavy Hydrocarbons in Supercritical Solvents," Ind. Chem. Fund., Vol. 18, 1979, pp. 149.

31. Peng, D.Y. and Robinson, D.B., "A New Two-Constant Equation of State," Ind. Eng. Chem. Func., Vol. 15, 1976, pp. 59.

32. Balenovc, Z., Myer, M.N., Giddings, J.E., "Binary Diffusion in Dense Gases to 1360 atmm by Chromatogrphic Peak-Broadening Method," J. Chem. Phys., Vol. 52, 1970, pp. 915.

33. Feist, R. and Schneider, G.M., "Determination of Binary Diffusion Coefficient of Benzene, Phenol, Naphthalene and Caffeine in Supercritical CO_2 between 308 and 333 ^{o}K in the Pressure Range 80 to 160 Bar with Supercritical Fluid Chromatography (SFC)," J. Separation Sci. and Tech., Vol. 17, 1982, pp. 261.

34. Waid, I. and Schneider, G.M., "Determination of Binary Diffusion Coefficients of the Benzene and Some Alkylbenzenes in Supercritical CO_2 between 308 and 320^{o}K in the Pressure Range 80 to 160 Bar with Supercritical Fluid Chromatography," Ber Bunsenges. Phys. Chem., Vol. 83, 1979, pp. 969.

35. Paulaitis, M.E., Krukonis, V.J., "Supercritical Fluid Extraction," Rev. Chem. Eng., Vol. 1, 1983, pp. 179.

36. Stephen, K. and Lucas, K., Viscosity of Dense Gas, Plenum Press, NY, 1979.

37. Carberry, J.J. and Bretton, R.H., "Axial Dispersion of Mass in Flow through Fixed Beds," AIChE J., Vol. 4, 1958, pp. 367.

38. Chung, S.F. and Wen, C.Y., "Longitudinal Dispersion of Liquid Flowing through Fixed and Fluidized Beds," AIChE J., Vol. 14, 1968, pp. 857.

39. Ebach, E.A. and White, R.R., "Mixing of Fluids Flowing through Beds of Packed Solids," AIChE J., Vol. 4, 1958, pp. 161.

40. Cholette, A. and Cloulier, L., ".", Can. J. Chem. Eng., Vol. 37, 1959, pp. 105.

41. Danckwerts, P.V., "Continuous Flow System (Distribution of Residence Time)," Chem. Eng. Sci., Vol. 2, 1953, pp. 1.

42. Wen, C.Y. and Fan, L.T., Models for Flow Systems and Chemical Reactors, Marcel Dekker, Inc., NY, 1975.

43. Sherwood, T.K. et al., Mass-Transfer, McGraw-Hill Inc., NY, 1975, pp. 136.

44. Kramers, H. and Alberda, G., "Frequency Response Analysis of Continyuous Flow Systems," Chem. Eng. Sci., Vol. 2, 1953, pp. 173.

45. Adler, R.J. and Hovorka, R.B., ".", JACC, Denver, 1961.

46. Deans, H.A. and Lapidus, L., "A Computational Model for Predicting and Correlating the Behavior of Fixed Bed Reactor: 1. Derivation of Model for Non-Reactive Systems," AIChE J., Vol. 6, 1960, pp. 656.

47. Levenspiel, O., "Mixed Models to Represent Flow of Fluids through Vessels," Can. J. Chem. Eng., Vol. 40, 1962, pp. 135.

48. Levenspiel, O., Chemical Reaction Engineering, John Wiley and Sons, NY, 1962.

49. Eckert E.R.G., Introduction to Heat and Mass Transfer, McGraw-Hill Inc., NY, 1950.

50. Debenedetti, P.G. and R.C. Reid, "Diffusion and Mass-Transfer in Supercritical Fluids," AIChE J., Vol. 32, 1986, pp. 2034.

51. Karabelas, A.J. et al., "Use of Asymptotic Relations to Correlate Mass-Transfer Data in Packed Beds," Chem. Eng. Sci., Vol. 26, 1971, pp. 1581.

52. Petrovic, L.J. and Thodos, G., "Mass-Transfer in the Flow of Gases through Packed Bed," Ind. Chem. Fund., Vol. 7, 1968, pp. 274.

53. Garner, F.H. and Grafton, R.W., ".", Proc. Roy. Soc. (London), Vol. A224, 1954, pp. 64.

54. McHugh, M. and Paulaitis, M.E., "Solid Solubilities of Naphthalene and Biphenyl in Supercritical Carbon Dioxide," J. Chem. Eng. Data, Vol. 25, 1980, pp. 326.

55. Goto, S. et al., "Mass Transfer in Packed Beds with Two-Phase Flow," Ind. Eng. Process Des. Dev., Vol. 14, 1975, pp. 473.

56. Morozov, V.S. and Vinkler, E.G., "Measurement of Diffusion Coefficients of Vapors of Solids in Compressed Gases. I. Dynamic Method for Measurement of Diffusion Coefficients," Russ. J. Phys. Chem., Vol. 49, 1975, pp. 1404.

57. Vinkler, E.G. and Morozov, V.S., "Measurement of Diffusion Coefficients of Vapors in Compressed Gases. II. Diffusion Coefficients of Naphthalene in Nitrogen and In Carbon Dioixde," Russ. J. Phys. Chem., Vol. 49, 1975, pp. 1405.

58. Iomtev, M.B. and Tsekhanskaya, Yu. V., "Diffusion of Naphthalene in Compressed Ethylene and Carbon Dioxide," Russ. J. Phys. Chem., Vol. 38, 1964, pp. 485.

59. Tsekhanskaya, Yu. V., "Diffusion in the System p-Nitrophenol-Water in the Critical Region," Russ. J. Phys. Chem., Vol. 42, 1968, pp. 532.

60. Schneider, G.M., "Chem. Thermodynamics Specialists Periodical Report," Tech. Report, Chem. Soc., London, 1978, Vol. 2, Chap. 4.

61. Gamson, B.W. et al., "Heat, Mass and Momemtum Transfer in the Flow of Gases through Granular Solids," AIChE J., Vol. 39, 1943, pp. 1.

U.S. DEPARTMENT OF COMMERCE
Technology Administration
National Technical Information Service
Springfield, VA 22161 (703) 605-6000